

Article

Techno-Economic Assessment of Offshore Wind Energy in the Philippines

Gerard Lorenz D. Maandal¹, Mili-Ann M. Tamayao-Kieke²  and Louis Angelo M. Danao^{3,*} 

¹ Energy Engineering Graduate Program, University of the Philippines, Diliman, Quezon City 1101, Philippines; gelomaandal@gmail.com

² Department of Industrial Engineering and Operations Research, University of the Philippines, Diliman, Quezon City 1101, Philippines; mmtamayao@up.edu.ph

³ Department of Mechanical Engineering, University of the Philippines, Diliman, Quezon City 1101, Philippines

* Correspondence: louisdanao@up.edu.ph

Abstract: The technical and economic assessments for emerging renewable energy technologies, specifically offshore wind energy, is critical for their improvement and deployment. These assessments serve as one of the main bases for the construction of offshore wind farms, which would be beneficial to the countries gearing toward a sustainable future such as the Philippines. This study presents the technical and economic viability of offshore wind farms in the Philippines. The analysis was divided into four phases, namely, application of exclusion criteria, technical analysis, economic assessment, and sensitivity analysis. Arc GIS 10.5 was used to spatially visualize the results of the study. Exclusion criteria were applied to narrow down the potential siting for offshore wind farms, namely, active submerged cables, local ferry routes, marine protected areas, reefs, oil and gas extraction areas, bathymetry, distance to grid, typhoons, and earthquakes. In the technical analysis, the turbines SWT-3.6-120 and 6.2 M126 Senvion were considered. The offshore wind speed data were extrapolated from 80 m to 90 m and 95 m using power law. The wind power density, wind power, and annual energy production were calculated from the extrapolated wind speed. Areas in the Philippines with a capacity factor greater than 30% and performance greater than 10% were considered technically viable. The economic assessment considered the historical data of constructed offshore wind farms from 2008 to 2018. Multiple linear regression was done to model the cost associated with the construction of offshore wind farms, namely, turbine, foundation, electrical, and operation and maintenance costs (i.e., investment cost). Finally, the levelized cost of electricity and break-even selling price were calculated to check the economic viability of the offshore wind farms. Sensitivity analysis was done to investigate how *LCOE* and price of electricity are sensitive to the discount rate, capacity factor, investment cost, useful life, mean wind speed, and shape parameter. Upon application of exclusion criteria, several sites were determined to be viable with the North of Cagayan having the highest capacity factor. The calculated capacity factor ranges from ~42% to ~50% for SWT-3.6-120 and ~38.56% to ~48% for 6.2M126 turbines. The final regression model with investment cost as the dependent variable included the minimum sea depth and the plant capacity as the predictor variables. The regression model had an adjusted R² of 90.43%. The regression model was validated with existing offshore wind farms with a mean absolute percentage error of 11.33%. The *LCOE* calculated for a 25.0372 km² offshore area ranges from USD 157.66/MWh and USD 154.1/MWh. The breakeven electricity price for an offshore wind farm in the Philippines ranges from PHP 8.028/kWh to PHP 8.306/kWh.



Citation: Maandal, G.L.D.; Tamayao-Kieke, M.-A.M.; Danao, L.A.M. Techno-Economic Assessment of Offshore Wind Energy in the Philippines. *J. Mar. Sci. Eng.* **2021**, *9*, 758. <https://doi.org/10.3390/jmse9070758>

Academic Editor: Liliana Rusu

Received: 15 June 2021

Accepted: 7 July 2021

Published: 9 July 2021

Publisher's Note: MDPI stays neutral with regard to jurisdictional claims in published maps and institutional affiliations.



Copyright: © 2021 by the authors. Licensee MDPI, Basel, Switzerland. This article is an open access article distributed under the terms and conditions of the Creative Commons Attribution (CC BY) license (<https://creativecommons.org/licenses/by/4.0/>).

Keywords: offshore wind; technical analysis; economic analysis; Philippines

1. Introduction

The Philippines adopted the Republic Act 9513 or An Act Promoting the Development, Utilization, and Commercialization of Renewable Energy Resources and for Other Purposes

on 16 December 2008 to pave the way for sustainable and affordable renewable energy [1]. The policies adopted in the Act are to accelerate the exploration and development of renewable energy resources, to encourage the development and utilization of such to reduce harmful emissions, and establish necessary infrastructure to carry out the mandate specified in the Act.

Under RA 9513, the National Renewable Energy Program (NREP) was formulated to provide the necessary framework for the country [2]. The main target of the NREP's energy policy is to increase the existing renewable energy capacity by 15.304 GW by 2030. The additional capacity is to come from wind, hydro, geothermal, solar, ocean, and biomass. Specific to wind energy, NREP's energy policy framework aims to achieve grid parity by 2025 through the addition of 2345 MW of capacity. However, only an additional 395 MW have been installed by 2015 and none thereafter [3]. A difference of 654 MW is required to reach the target for that same year. This backlog is indicative of the slow pace of development in the Philippines so that the target grid parity will not be realized as envisioned. Other pathways to achieve this goal are necessary and venturing into the offshore wind arena may be a viable option.

Offshore wind farms (OWF) have gained attention in the past years due to some inherent advantages present. Capacities of OWF are significantly greater than their onshore counterparts, sometimes reaching 1000 MW [4]. The wind resource in the ocean is less intermittent than on land and can be predicted with greater accuracy [5]. Furthermore, social acceptance is greater for OWF due to low visual and noise impact [4]. To assess these, the technical and economic viability of OWFs in the Philippines was studied in this work.

1.1. Statement of the Problem

As of 2015, the Philippines has not achieved its target capacity for wind energy installations by 62%. OWFs are investigated and considered in this research to possibly fill in the gap in the capacity. Specifically, the technical and economic aspects of OWFs were studied for their viability in the Philippine setting. As a caveat, there are difficulties in the assessment of OWFs in the Philippines, which are stated below:

- Methodologies on techno-economic assessment of offshore wind energy have not been applied to the Philippine setting.
- A notion exists that it is a risky investment with high cost and uncertainty in return.
- There is no readily available and reliable information for investments regarding the viability of offshore wind farms in the Philippines.
- There has been no formulation for the recommendation of the viability of offshore wind energy in the Philippines.

1.2. Objectives of the Study

The main objective of the study was to develop a framework in assessing the technical and economic potential of offshore wind energy in the Philippines. It aims to achieve the following specific objectives:

- To develop a methodology for the techno-economic assessment of offshore wind farms in the Philippines.
- To assess the wind resource in the Philippine oceans for the potential of putting up an offshore wind farm.
- To investigate the economic viability of constructing an offshore wind farm in the Philippines through *LCOE*.
- To formulate a recommendation for the viability of OWF in the Philippines.

1.3. Research Significance

The current pace of development of wind energy in the Philippines is slow in terms of attaining grid parity in wind energy with the commissioning of 2345 MW of additional capacity by 2030. The bulk of the commissioning of wind power plants was done in 2014 under four projects with a total capacity of 303.90 MW [3]. In 2015, there were only two

projects constructed with a combined installed capacity of 90 MW [6,7]. By exploring the emerging technology of offshore wind energy, higher capacity wind farms can be built with the availability of space and good wind resource. This techno-economic assessment research can help assess the viability of the construction of an offshore wind farm in the Philippines. The investors and government may benefit from this study since they will be able to see the technical and financial model of the study wherein the *LCOE* and price of electricity are included. These economic measures may give the investors an option to consider offshore wind farms as one of their investments and provide the government insights for the promotion of this emerging renewable energy technology.

The novelty of this research compared to existing technical and economic assessment of offshore wind farms is the extensive application of exclusion criteria, comparison of two offshore wind turbines, and rigorous economic analysis in the Philippines setting.

1.4. Limitations of the Study

Since offshore wind energy is an emerging technology around the world, there are various improvements that can be adopted in this research in terms of technical and economic data acquisition. The accuracy and reliability of the results in the technical potential of offshore wind is heavily dependent on the data at reference height, spatial resolution, and time interval. The available data acquired by the researcher are from the Phil-LiDAR 2 Program of the Department of Science and Technology with a spatial resolution of 4 km, and mean wind speeds for five years at 10 m, 20 m, 80 m, and 100 m elevations.

The data for the economic analysis were acquired from 4C Offshore. The offshore wind farms considered were the ones constructed from 2008 to 2018. The data acquired include the name of the power plant, country of origin, minimum and maximum sea depth, area, offshore cable length, onshore cable length, inter-array cable length, port for O&M, distance from port, turbine model, number of turbines, turbine capacity, plant capacity, and investment cost. Offshore wind farms with incomplete data were not considered in the study.

Since the different parts of the Philippines have varying wind speeds, only a selected site with the highest capacity factor will be considered for the economic analysis. In this study, the offshore wind energy will be compared to the price of onshore wind farms in terms of investment cost and price of electricity since onshore wind is a renewable energy technology with a share of 3.57% of the total installed capacity in the Philippines, respectively [3].

The stationary foundation technologies, namely, monopile, jacket, and tripod, will be the interest of this research due to its high capacity production at stationary structures. Thus, the limitation of the study was within 50 m bathymetry.

2. Review of Related Literature

2.1. Offshore Wind Farms

There are numerous advantages of offshore wind farms that address the disadvantages of putting up an onshore wind farm. Wind farms, in general, emit noise mostly from the rotation of blades [8]. In some cases, the annoyance from the noise coming from onshore wind farms can lead to psychological distress and sleep disturbance to the people living within the vicinity of wind turbines [9]. With the offshore wind farm situated in the ocean, low noise is heard [4].

Offshore wind farms have a more stable wind production compared to onshore wind farms. The power duration curve of offshore wind power plants is greater than onshore wind farms in Germany [5]. Higher and steadier offshore wind farms are more productive in the UK with a 36% capacity factor compared to onshore wind farms (27% capacity factor), which implies a higher capacity credit and smaller back-up cost [10].

Forecasting of wind energy is another concern in wind energy technology due to the intermittency in wind resources. In the case of offshore wind farms, wind energy can be

predicted with a relatively smaller error compared to onshore wind farms. Offshore wind farms need fewer reserves in the balancing of forecast error [5]. The results of the study of Richts et al. [5] illustrate that offshore wind farms can have more than 50% of their power output predicted with 99.994% reliability in one-hour advance compared to onshore wind farms with only about 30% power output predicted with the same level of reliability.

A study showed that the proximity of wind turbines near residence areas negatively influences attitudes toward installations. However, with proper consultations and proper participatory siting, wind farms can receive a higher level of acceptance [11]. Through proper consultations with the affected stakeholders and participatory siting, the possibility of the construction of an offshore wind farm can also be accepted.

2.2. Offshore Wind: Current Status

2.2.1. Installed Capacity

Rapid increase in offshore wind farms has been evidently seen for the past two decades in Europe. The total installed capacity for offshore wind farms was only 50 MW in 2000 and increased up to 1471 MW by the year 2008, which means an annual growth of approximately 50% [10]. In 2016, the total installed capacity in Europe reached 12,631 MW [12].

In 2006, the average wind farm size in Europe was only 46.3 MW. After 10 years, the average size has increased up to 379.5 MW based on offshore wind farms under construction in 2016 [12]. Offshore wind farms have high potential to have larger size capacity as planned in Europe.

2.2.2. Number of Turbines and Project Area

The project average area and number of turbines of commissioned and under construction offshore wind farms in Europe was studied extensively [13]. It was seen that the project area in 2015 was lower compared to 2012, but the average size was higher than in 2012. The developments in the turbine industry can explain this event as the turbines have increased in capacity and the number of turbines has also increased.

2.2.3. Distance to Shore and Water Depths

In European installations, the distance to shore vs. water depth was studied [12]. As the distance of the offshore wind farm to the shore increases, it also translates to a higher installed capacity. There is a rapid increase in the distance to the shore as time goes by [11]. In 2013, the average distance was just 25 km, but it has rapidly increased to an average distance of 42 km to the shore.

2.2.4. Cost

There has been an increase in the CAPEX despite the technological advances in offshore wind energy [13]. The annual construction of deeper and farther offshore may contribute to the rise of CAPEX since these factors increase the grid connection, foundation, and installation costs.

2.2.5. Wind Turbines

The wind turbine is an important parameter in the construction of offshore wind farms. In Europe, the average capacity rating was 4.8 MW based on 361 offshore wind turbines that are in the progress of being constructed in 2016 [12]. It was seen that the progression of rated capacity gradually increases from 0 MW to 4.9 MW in 20 years. Among the different offshore wind turbine manufacturers in Europe, Siemens Wind Power was the biggest supplier with 67.8% installed capacity [12].

2.3. Foundation Technologies

There are proven and tested stationary foundations within 50 m of depth, namely, monopile, jacket, and tripod [14]. The floating structures are considered optimal for bathymetry greater than 50 m, namely, tension leg platform, semi-submersible, and spar

buoy [15]. The stationary foundation technologies will be the interest of this research due to its high capacity production at stationary structures.

2.4. Renewable Energy Law in the Philippines

The Republic Act No. 9513, also known as the “Renewable Energy Act of 2008”, is an act promoting the development, utilization, and commercialization of renewable energy resources and for other purposes. In this law, policies and regulations are enacted to favor the utilization of renewable energy technologies in the Philippines such as wind energy. A feed-in tariff system is applied to renewable energy technologies to leverage them from the wholesale electricity spot market by prioritizing their connection to the grid, prioritizing for their purchase and transmission or “priority dispatch”, fixed tariff for up to 20 years, and has a mandated minimum percentage of generation.

Aside from the feed-in tariff system that promotes renewable energy technologies, tax incentives are included in this law. Renewable energy power plants can have income tax holiday for the first seven years of the power plant, duty-free importation of machinery, equipment, and materials for the first ten years, and a 10% corporate tax rate instead of 30% [1]. With these policies enacted, the chances of constructing an offshore wind farm can increase, but the technical and economic aspects should still be investigated.

2.5. Related Techno-Economic Studies

The technical and economic feasibility of OWF in Chile were studied by Mattar and Guzmán-Ibarra [16]. The Vestas V164 8.0 MW wind turbine was studied using wind data from the ERA-interim reanalysis spanning the years 1979 to 2014. Performance and capacity factor were calculated for wind speeds extrapolated from 10 m above sea level. Information on costing was obtained from previous studies involving the full life cycle of wind farms and used in the economic analysis of the study. Estimates for a useful life of 25 years were computed for the levelized cost of electricity (LCOE), payback period, internal rate of return, and net present value. Three capacities were considered to estimate the LCOE. These were 80 MW, 160 MW, and 240 MW.

Power density maxed at 3190 W/m² with the capacity factor of 70% and LCOE between 72 and 100 USD/MWh for locations between 45° and 56° S. Rated at 13 m/s, the best location for the selected wind turbine was shown to be between 30° and 32° S. Power density at that location was between 700 W/m² and 900 W/m² with capacity factor ranging from 40 to 60%. The LCOE values were seen to range from 100 to 114 USD/MWh. It was determined that an increase in discount rate by only 2% can increase the LCOE threefold.

The techno-economic and environmental considerations of OWF along India’s coastline were studied by Nagababu et al. [17] using a geospatial information system (GIS). Cost supply curve and spatial distribution of levelized production cost (LPC) were created and sensitivity analyses were carried out to examine the effect of project lifetime, annual energy production, availability, and discount rate on cost.

Results revealed a wide range of wind power densities for both east and west coasts. The western coastline sees power densities from 13 to 294 W/m² while the eastern coastline gets power densities of 63 to 393 W/m². Theoretically, these translate to annual energy potential ranges of 54 to 823 MWh/km² and 107 to 1117 MWh/km² for the western and eastern coast, respectively. Compared to existing renewable energy resources in India within the 200 Euro/MWh FIT, a good 40% of the potential is available that is economically competitive. Bottom fixed wind farms in the western coastline will produce energy at costs of 231 and 262 Euro/MWh for 0 to 30 m and 30 to 50 m depths, respectively. The eastern coastline will see higher costs for similar installations at 308 and 334 Euro/MWh for 0 to 30 m and 30 to 50 m depths, respectively. Interest rate was seen as a very influential parameter for the calculation of the LPC.

Khraiwish Dalabeeh [18] studied the cost of energy and capacity factor of OWF at five prospective locations in Jordan by developing a simulation model using Weibull parameters

and computing for annual generation of different wind turbine models. The most suitable wind turbine was matched to the locations studied and the cost of electricity and capacity factors were determined subsequently. Nine years' worth of wind data were utilized for the analysis of the prospective sites.

The analysis showed that there were five suitable sites that have good wind resources for electricity generation. The Xemc-Darwind was observed to produce the lowest cost of electricity at 25.9 USD/MWh. Aaer and Acciona produced the greatest cost at 100 to 222 USD/MWh for sites Der Alla, Amman, and Irbid due to low wind resource and high property prices. R. Monif came out to be the most suitable site for the deployment using the Xemc-Darwind rotor with the least cost of electricity at 25.9 USD/MWh and highest capacity factor of 42%. Fossil fuel power generation costs in 2013 were significantly higher than the computed wind energy generation cost with an average of 260 USD/MWh.

Schweizer et al. [19] conducted the first feasibility study of the offshore wind farm in the coast of Rimini at the Northern Adriatic Sea. The wind speed data were acquired in 2008 to 2013 through the anemometers mounted on a gas platform, and the characteristics of the wave were analyzed through the data using a wave buoy installed in 2007 (located few kilometers at the study area). The study also described the environmental external conditions that could potentially act on the offshore wind farm and are crucial for the engineering design. A commercially available wind turbine was selected in the study with a rated power of 3.6 MW, and the capacity factor was calculated to be 25% using the experimental wind probability distribution at 80 m above sea level. It was found that for layout A (15 wind turbines, 54 MW installed capacity), the best case had 97% WT availability, 9.75% internal losses while the worst case had 90% WT availability, 11% internal losses, and 0.205 €/kWh feed-in tariff. For layout B (60 wind turbines, 216 MW installed capacity, 0.160 €/kWh feed-in tariff), the best case had 97% WT availability, 9.75% internal losses, and 0.205 €/kWh feed-in tariff, while the worst case had 90% WT availability, 11% internal losses, and 0.160 €/kWh feed-in tariff. It was seen that the assumed feasibility study and commissioning will last up to four years with the offshore wind farm to be operational in 25 years, while the last year is for decommissioning. In all of the cases, positive net cash flow can be seen. The lowest net income was found in layout A in the worst case scenario, and the most adequate result in terms of finance could be found in layout B with the best case scenario.

Cavazzi and Dutton [20] studied the potential of offshore wind energy in the UK with the aid of GIS. A suitability map was produced taking into account technical and economic factors that influence the OWF potential of the study area. Certain sites were excluded based on specific constraints applied such as existing offshore installations, submarine cables, oil and gas extraction areas, among others. The LCOE was calculated and a sensitivity analysis was conducted to ascertain which factors greatly influence the LCOE. It was observed that the interest rate contributed the most in influencing the LCOE. Of the available offshore wind resources in the UK, 10% is potentially accessible for a 150 GW wind farm that will produce energy at a cost of less than 140 Euro/MWh.

2.6. Exclusion Criteria

The Philippines is composed of 7641 islands, and there are three main island groups, namely, Luzon, Visayas, and Mindanao. Since the Philippines has more than 7000 islands, there is a need to narrow down the sites that could have the potential for the construction of an offshore wind farm. With this premise, the study excludes sites if they do not meet the certain constraint criterion. In the study of the multi criteria decision analysis of offshore wind energy potential in Egypt, the constraints considered for site exclusion are distance from shore, depth, submerged cable paths, oil and gas extraction areas, shipping routes, nature reserves, and military areas [21]. The constraints considered in the study on the assessment of the UK's offshore wind energy potential by using geographic information systems were anchorage areas, existing wind farms, active submarine cables, protected wrecks, sand mining, IMO traffic separation schemes, and oil and gas extraction areas [20].

For this study, the constraints considered for excluding sites are active submerged cable paths, local ferry routes, marine conservation areas, reefs, oil and gas extraction areas, depth, and distance from grid. Since the Philippines is located in the Pacific Ring of Fire, it is susceptible to calamities. The other constraints that will be considered are typhoons and earthquakes.

Active submerged cables are used for transmitting data through the use of cables laid on the seabed. These are essential for the telecommunications industry in transmitting data to connect with other countries and also to connect to the Internet. These cables can reach up to 9000 km in length with a price of \$300,000 USD [22]. In this study, the path of active submerged cables with a buffer of 5 km were excluded in the siting process of the offshore wind farm. The active submerged cable map was acquired from Submarine Cable Map [23].

Local ferry routes in the Philippines were generated by Thierry Crevoisier for the World Food Program on 25 February 2014 [24]. In this study, the local ferry routes in the Philippines were excluded in the siting process since these offshore wind farm may pose safety concerns along the path. A buffer of 3 km was applied when using this criterion.

According to the Republic Act 7586, also known as the “National Integrated Protected Areas System Act of 1992”, protected areas are identified as areas of water and land that are set aside for preservation due to its unique biological and physical significance, managed for the improvement in biodiversity, and protected from destructive human exploitation [25]. The National Integrated Protected Areas System (NIPAS) is tasked to manage the preservation of the protected areas. The following are categorized as protected areas, namely, strict nature reserve, natural park, natural monument, wildlife sanctuary, protected landscapes and seascapes, resource reserve, and natural biotic areas. In this study, all protected areas were excluded [26]. The marine protected areas are the areas with a dark shade of blue in the map. A buffer zone of 3 km was applied based on a study that 90% of marine protected areas were less than 1 km² [27].

The Philippines is part of the Coral Triangle with Malaysia, Timor-Leste, Indonesia, Papua New Guinea, and the Solomon Islands. This group of countries contain one-third of the world’s coral reefs [28]. Coral reefs act as the main buffer against erosion due to typhoons and waves, and it also serves as houses for the fish in the ocean [29]. The data on the location of coral reefs in the Philippines is based on ReefBase, which serves as the official database of the International Coral Reef Action Network and Global Coral Reef Monitoring Network [30]. Locations with coral reefs are excluded in the analysis. The coral reef areas are indicated by the dark brown shade in the map. Similar to marine protected areas, a buffer area of 3 km was applied in the exclusion of coral reefs.

The Department of Energy contracts private companies to extract oil and gas in the vicinity of the country. The map for the oil and gas extraction areas was acquired from the Department of Energy [31]. These oil and gas extraction areas reach up to 1,476,000 hectares such as in the case of BHP Billiton in Southwest Palawan. The areas that have already contracted and the areas up for contracting for around 5 km will be excluded from the study.

The depth of the ocean or the bathymetry affects the type of foundation to be applied and the economic cost of the offshore wind farm. The type of foundation technology to be used in this study is a stationary foundation since it can be applied within a depth of 50 m [14]. There is an increase in the CAPEX as the depth also increases [13]. The map for the depth of the ocean in the Philippines was acquired from the General Bathymetric Chart of the Ocean [32]. The bathymetry excluded in this study were depths greater than 50 m.

As the distance from the grid to the offshore wind farm increases, the transmission cost also increases related to grid connection [20]. The distance greater than 120 km from the grid will be excluded from the analysis since longer distance may yield high uncertainty with the cost. The data for the transmission lines was acquired from National Renewable Energy Laboratory [33].

In the study by Worsnop et al. [34], they predicted that offshore wind turbines cannot withstand hurricane gusts of up to 90 m/s (324 km/h)—modern wind turbines can only withstand gusts of up to 70 m/s (252 km/h) based on engineering standards. In the Philippine context, tropical cyclones reach up to a maximum of 250 km/h according to the United Nations Office for the Coordination of Humanitarian Affairs [35]. However, there are only limited studies regarding the impacts of tropical cyclones to offshore wind farms, and this could be a potential area of research for the improvement of these offshore wind turbines. Due to the limitation on the studies in tropical cyclone impacts, wind speed of gusts greater than 250 km/hour will be excluded in the study. The buffer area considered in the application of typhoon path was 50 km since the maximum wind speeds were within the eye wall with a maximum distance of 50 km [36,37].

In 2011, the Kamisu offshore wind farm in Japan was struck by an earthquake with an epicenter distance of 300 km and a magnitude of 6 [38]. The 2 MW offshore wind farm survived the disaster, and was even operational after three days. The Kamisu offshore wind farm is located 40 m from the coast with a monopile foundation technology. One of the solutions of the Niras international engineering consultancy regarding earthquake and typhoon problems is the application of a jacket foundation, which is built on a grid construction of steel placed on four piles [39]. A possible option for offshore wind farms is jacket foundations, which are more robust with regard to the size of the foundation at a greater ocean depth. In this study, a buffer of 15 km from the high historical earthquakes will be applied based on the 10 km critical damage to a dyke of a 7.8 magnitude earthquake in Japan [40].

2.7. Wind Curtailment

It is a challenge if there is a high level of penetration from wind energy to the grid due to its limits in predictability and variability. Wind energy may be curtailed when there is a lack of available transmission, system balancing issues, or back-feeding. Wind curtailment is referred to as the utilization of less wind at a certain time even though there is still more wind power potential available [41].

In 2013, China's installed wind capacity was 77.16 GW with 142 TWh generated electricity or 2.6% of the total electricity generated in the country [42]. In that same year, it curtailed 16.23 TWh of wind energy or 10.74% of the total wind energy generated. Some parts of the country had higher wind curtailment such as in Jilin and Gansu with 21.79% and 20.69%, respectively. High concentration of wind farms in northern and northwestern parts of China, but low electricity demands have contributed to the curtailment. The transmission capacity to deliver electricity to different parts of China with high demand is also insufficient. Some other factors for wind curtailment are also guaranteed minimum dispatch for coal plants and the need for combined heat and power plants during winter for heating. China's solution to wind curtailment is an improvement in forecasting and scheduling, construction of dispatch system for wind power, utilization of automatic generation control systems (AGC), and the application of electric boilers powered by wind energy.

In Denmark, there was an additional installed capacity of 4893 MW in 2014 that produced electricity of 13.1 TWh (1272 MW and 5.2 TWh are from offshore wind farms) [42]. The wind integration in this country is reinforced by the interconnection of systems to neighboring countries with an international electricity market. For instance, over-generation of wind energy is avoided through negative price signals in the day-ahead and intra-day power market. Large capacity offshore wind farms negotiate through the tendering process for compensation.

The United States of America has numerous balancing areas in different parts of the country. The wind curtailment is generally less than 4% [42]. The factors affecting wind curtailment are excessive wind energy during low demand periods and during requirements of minimum generation such in the case of Bonneville Power Administration (BPA) and the Electric Reliability Council of Texas (ERCOT).

The wind curtailment in different countries was also reported by Bird et al. [42]. The data for Germany dated to 2012. The electricity generation from wind ranges from 0.4% to 31.9%. Globally, wind curtailment ranges from 1% to 3% with the exception of 11% in China.

2.8. Data Sources

The data acquired for the wind speed are from Phil-LiDAR 2 Program of the Department of Science and Technology with a 4 km spatial resolution and distance of 10 km from the shore [43]. The offshore wind data are an annual wind speed at elevations of 10 m, 20 m, 80 m, and 100 m in 2008, 2010, 2014, 2015, and 2016, respectively.

2.9. Technical Analysis

2.9.1. Power Law

An important parameter for the assessment of wind power potential in a specific site is the reference height of the wind speed data. Nowadays, wind turbine heights range from 50–120 m [44]. More reliable results can be acquired if the reference height of the wind speed data is close enough to the hub height.

The mathematical model for power law can be seen in Equation (1) where v_1 (m/s) is the wind speed at reference height z_1 (m); v_2 (m/s) is the wind speed at height z_2 ; and z_0 is the roughness length factor. An established value of 0.0002 m is used, which corresponds to sea surface [16,17].

$$v_2 = v_1 \frac{\ln \left[\frac{z_2}{z_0} \right]}{\ln \left[\frac{z_1}{z_0} \right]}. \quad (1)$$

2.9.2. Weibull Model

There are two known statistical approaches for calculating wind power potential, namely, the Weibull and Rayleigh Distribution models. Based on the study of Celik [45], the Weibull model gives better performance compared to the Rayleigh model based on monthly fitness coefficients in calculating the wind power potential in Iskenderun, Turkey. However, due to limitations in the type of data acquired, the Weibull model was used with a shape parameter value of 2, effectively reducing it to the Rayleigh model.

The mathematical model for the estimation of the wind power potential can be calculated from the Weibull distribution model in Equation (2) with $p(V_2)$ as the Weibull probability density; k as the shape parameter (dimensionless); c as the scale parameter (m/s); and v_2 as the wind speed (m/s) [44]. The assumed value of the shape parameter based on another study is 2 [20].

$$p(V_2) = \left(\frac{k}{c} \right) \left(\frac{v_2}{c} \right)^{k-1} \exp \left[- \left(\frac{v_2}{c} \right)^k \right]. \quad (2)$$

2.9.3. Wind Turbine Power Curve

The SWT-3.6-120 manufactured by Siemens and the 6.2M126 manufactured by Senvion were used in the study. The SWT-3.6-120 with a 3.6 MW optimal output was utilized in the analysis because of its high tolerance to wind gusts of up to 70 m/s. It has a 120 m rotor diameter with a cut-in wind speed of 3–5 m/s, nominal power at 12 m/s to 13 m/s, and cut-out wind speed of 25 m/s based on the manufacturer's datasheet [46]. The data were digitized from the published power curve for the technical analysis of the annual wind energy production from 0 to 25 m/s.

The Senvion 6.2M126 has a rated output of 6.15 MW, and it is used to check the effects of having a high capacity with respect to net present value, payback period, internal rate of return, and levelized cost of electricity. It has a 126 m rotor diameter with a cut-in wind speed of 3.5 m/s, nominal wind speed at 13.5 m/s, and cut-out wind speed of 30 m/s based on the manufacturer's datasheet [47]. The data were digitized from the published

power curve for the technical analysis of the annual wind energy production from 0 to 30 m/s.

2.9.4. Wind Power and Wind Power Density

The wind power density is the power per area that can be harnessed from the specified site, which can then be computed from the wind speed data and probability density curve. The formula for wind power density can be seen in Equation (3) with P/A as the wind power density (W/m^2); P as the wind power (W); A as the swept area (m^2); ρ as the air density ($1.225\text{ kg}/m^3$); $p(V_2)$ as the wind probability density; and V_z as the magnitude of the wind speed (m/s) [16].

$$\frac{P}{A} = 0.5\rho \int_0^\infty V_2^3 p(V_2) dV. \tag{3}$$

2.9.5. Annual Wind Energy Production

The annual wind energy production is the energy that is harnessed from the site. The formula for annual wind energy production E can be seen in Equation (4) with T as the time period of the study (8760 h); $p(V_2)$ as the Weibull probability density; and $P(V_2)$ as the wind turbine power output corresponding from the wind turbine curve [16].

$$E = T \int_0^\infty p(V_2) P(V_2) dV. \tag{4}$$

2.9.6. Capacity Factor

The capacity factor is the ratio between the wind power generation from the turbine and the total power generation it produces at full capacity in a period of time. The equation for capacity factor CF can be seen in Equation (5) with PE as the estimated output; PN as the rated output; and T as the time period [13]. The generally accepted values for offshore wind capacity factor are in the range between 30% and 55% [48].

$$CF = \frac{PE}{PN(T)}. \tag{5}$$

2.9.7. Performance

The annual seasonal performance is the ratio between the wind energy produced by the turbine and the energy that is possessed by the wind annually. It shows the relationship between the wind turbine and the wind energy in the location. The equation for the performance of a turbine is shown in Equation (6) with η_{EST} as the wind turbine’s seasonal performance; E as the wind energy produced; and E_d as the energy possessed by the wind. The considered technically viable performance for the wind turbines in this study is greater than 10% [16].

$$\eta_{EST} = \frac{E}{E_d}. \tag{6}$$

2.9.8. Array Spacing and Number of Turbines

The number of turbines for the areas that are viable for the technical aspect and exclusion criteria are dependent on the total available area and array spacing, as seen in Equation (7) [49,50]. The array spacing is estimated using the rotor diameter, downwind spacing factor, and crosswind spacing factor as seen in Equation (8) [21,49,50]. Values of 10 and 5 were applied to the downwind and crosswind spacing factors, respectively, to reduce the inter-turbine wake losses.

$$\text{Number of Turbines} = \frac{\text{Total Available Area}}{\text{Array Spacing}}. \tag{7}$$

$$\text{Array Spacing} = (\text{Rotor diameter})^2 \times \text{Downwind Spacing Factor} \times \text{Cross Wind Spacing Factor}. \tag{8}$$

2.10. Economic Analysis

2.10.1. Investment Cost

The investment cost of an offshore wind farm has commercial sensitivities, which makes the estimation difficult. The components of total capital cost such as wind turbine and electrical costs are acquired from different sources. The summation of all the total capital costs C_{Total} can be seen in Equation (9) with C_{WT} as the wind turbine cost; C_F as the foundation cost; C_E as the electrical cost; and other costs such as operation and maintenance [17].

$$C_{Total} = C_{WT} + C_F + C_E + Other\ cost. \quad (9)$$

The data acquired for the cost components of offshore wind farms were from “4COffshore”, which is a market research and consultancy organization that focuses on offshore energy markets, and it has been cited in numerous studies [51–53]. The offshore wind farms that are constructed from 2008 to 2018 only were considered in the study. The data acquired from “4COffshore” were the name of the power plant, country of origin, minimum and maximum sea depth, area, offshore cable length, onshore cable length, inter-array cable length, port for O&M, distance from port, turbine model, number of turbines, turbine capacity, plant capacity, and investment cost.

2.10.2. Multiple Linear Regression

In this study, different cost parameters are considered to quantify each component of the investment cost using multiple linear regression as seen in Equation (10), where Y is the investment cost component; $\beta_{j,j} = 0, 1, 2, \dots, k$, are the regression coefficients; $x_{j,j} = 0, 1, 2, \dots, k$, are the predictor variables; and ε is a random error term [54]. The predictor variables considered were date commissioned, type of foundation, hub height, sea depth, minimum distance from shore, useful life, offshore cable length, onshore cable length, inter-array cable length, distance from port, distance from grid, turbine size, number of turbines, and capacity. The estimated investment cost of existing offshore wind farms around the world for the last ten years were considered.

$$Y = \beta_0 + \beta_1x_1 + \beta_2x_2 + \dots + \beta_kx_k + \varepsilon. \quad (10)$$

The coefficient of determination (R^2) was investigated using the statistical software to acquire the best multiple linear regression model. The coefficient of determination or the R^2 is a measure of the goodness-of-fit of the regression model. The highest and greater than 80% value will be applied to the economic analysis of the study.

The mean absolute percentage error ($MAPE$) of the model was analyzed, which aims to validate results. The $MAPE$ is a measure of the quality of the regression model [55] and measures how close the predicted values of the regression model are to the target variables.

2.10.3. Multiple Regression Assumptions

There are four assumptions in multiple regression analysis for the regression model to be valid. These four assumptions are normality, linearity, homoscedasticity, and reliability of measurement. If these assumptions are not satisfied, the results may be deemed inaccurate and may also result to type I or type II errors [56].

The assumption of normality implies that the distribution of the dependent variables and independent variables are normal. This can be checked through visual inspection of the residuals. A q–q plot can be done to visually check the normality of the variables. A model is considered a good model for normality if the residuals do not deviate largely from a straight line, while a bad model would show a large deviation from a straight line [57].

The assumption of linearity indicates that there is a linear relationship between the independent and dependent variables. A further visual inspection of the scatterplot of the residuals can be done to determine whether there is a linear pattern or not. A model is considered a good model for a linearity if there is equal distribution of the residual across a horizontal line through 0, while a bad model will show a curvilinear pattern [57].

Homoscedasticity implies that the variance of errors is the same across all independent variables. In the case of heteroscedasticity, there are different variance of errors from different values of the independent variables. The assumption for homoscedasticity can be satisfied by checking if the residuals are equally distributed along the predicted values. A model is considered homoscedastic if it appears to be randomly spread out a horizontal line while a model is heteroscedastic if there is a wider spreading of residuals along the x -axis, leading to a steep line fitted through [57].

A good reliability of measurement for multiple regression indicates that the effect sizes of other variables should be minimized. It also implies that there should be no multicollinearity, or the independent variables should not be highly correlated with each other because this may lead to over estimation. A residual vs. leverage plot may help in searching for influential observations that do not follow the trend of most other observations, and the variance inflation factor (*VIF*) is a method for checking the correlation of independent variables. A reference line called the Cook's distance is added and observations outside this line are considered influential observations outside the trend [57]. Observations outside should be omitted since they influence the resulting slope coefficient and R^2 significantly. In the *VIF* method, independent variables with greater than 5 values indicate that there is multicollinearity with each other and should be omitted carefully.

2.10.4. Net Present Value

Net present value (*NPV*) is an economic metric to indicate the total benefit from an investment. It is a measure of the incoming and outgoing cash flow in the investment as seen in Equation (11), whereas the N is the number of years from zero to the last year of the investment; FC is the cash flow for an annual period reaching the last year of the investment; and r is the discount rate. A *NPV* greater than zero means that the investment is profitable, while a *NPV* less than zero is not profitable, and the investment should not be pursued. If the *NPV* is exactly zero, nothing has been gained or lost, which means the project should also not be pursued [16].

$$NPV = \sum_{t=0}^N \frac{FC_t}{(1+r)^t} = v_1 \frac{\ln \left[\frac{z_2}{z_0} \right]}{\ln \left[\frac{z_1}{z_0} \right]}. \quad (11)$$

2.10.5. Levelized Cost of Electricity

Levelized cost of electricity (*LCOE*) is a general measure for the evaluation of the life cycle cost of a power plant. It can also be used for the comparison of different power plant technologies in terms of its life cycle cost and energy production. It accounts for the total installation cost, annual operation and maintenance, and energy production [58].

The formula for *LCOE* can be found in Equation (12) with I_T is the investment at time t ; M_T is the operating and maintenance cost at time t ; E_T is the energy produced (MWh) at time t ; r is the discount rate (%); and t is the time from base year up to the total number of years of operation [16].

$$LCOE = \frac{\sum_{t=0}^n \frac{I_T + M_T}{(1+r)^t}}{\sum_{t=0}^n \frac{E_T}{(1+r)^t}}. \quad (12)$$

3. Methodology

The methodology described in this study focused on two aspects of the potential siting of an offshore wind farm, namely, the technical and economic aspects. In the succeeding chapters, the framework of the methodology of the study will be discussed together with its detailed procedures. The methodologies were aligned with the objectives of the study found in Section 1.2.

The novelty of this research compared to existing technical and economic assessment of offshore wind farms are the application of numerous exclusion criteria, comparison

of two offshore wind turbines, and rigorous economic analysis in the Philippines setting. Compared to other techno-economic assessment studies, nine exclusion criteria were applied in this study to exclude areas that are not suitable as a potential site for offshore wind farms. Calamities such as historical earthquakes and typhoons have been considered as exclusion criteria. In the technical analysis, two turbines have been considered, namely, the SWT-3.6-120 and 6.2M126 turbines. In other techno-economic studies, they have considered only one turbine. The economic analysis done in this study covers the actual costs of offshore wind farms around the world for the period 2008 to 2018. These data were then used to generate a multiple regression model to capture the investment costs of offshore wind farms. The levelized cost of electricity and the price of electricity of offshore wind farms in the Philippines were taken into account. In other techno-economic studies, they only considered the levelized cost of electricity. Finally, the novelty of this study is that analysis was done with relevant assumptions in the Philippines. It is also the first available and published technical and economic assessment of offshore wind farms in the Philippines that follows engineering methods.

3.1. Framework of Methodology

The flow diagram of the methodology is shown in Figure 1. The framework has three stages: data gathering, exclusion analysis, and technical and economic analysis. The acquisition of data included methods of the recent research work on techno-economic analysis of OWE, collection of wind speed data, and developing the simulation model using GIS. The application of the exclusion criteria not only narrowed down the locations of potential sites, but more importantly, masked out all of the unsuitable sites in the Philippines due to restrictions by local legislation and current global offshore industry practice. Subsequently, the suitable sites were then subjected to technical and economic analysis.

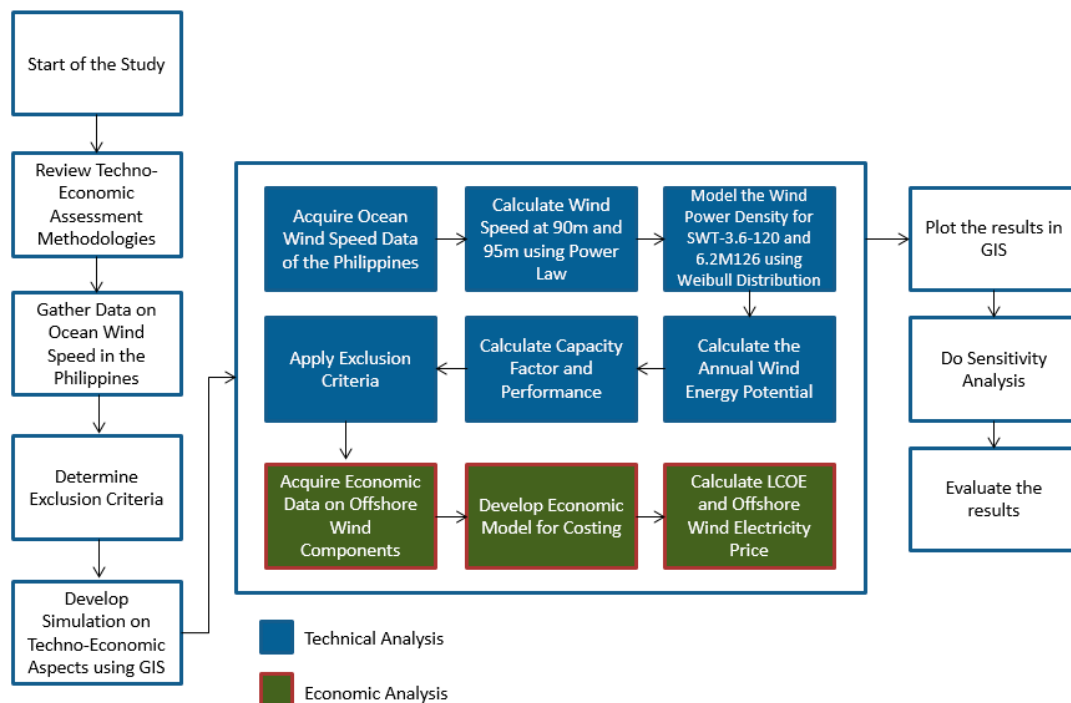


Figure 1. Framework of methodology.

3.1.1. Exclusion Criteria

The constraints considered in this study are presented in Figure 2. Using the raster method in GIS, all constraints were overlaid in the wind resource map to exclude these

areas as unsuitable locations in the analysis. It should be noted that the suitability of the locations was determined purely by technical and economic considerations in the study. The exclusion step was applied to reduce the potential sites with no consideration to linearized scoring of factors that affect suitability.

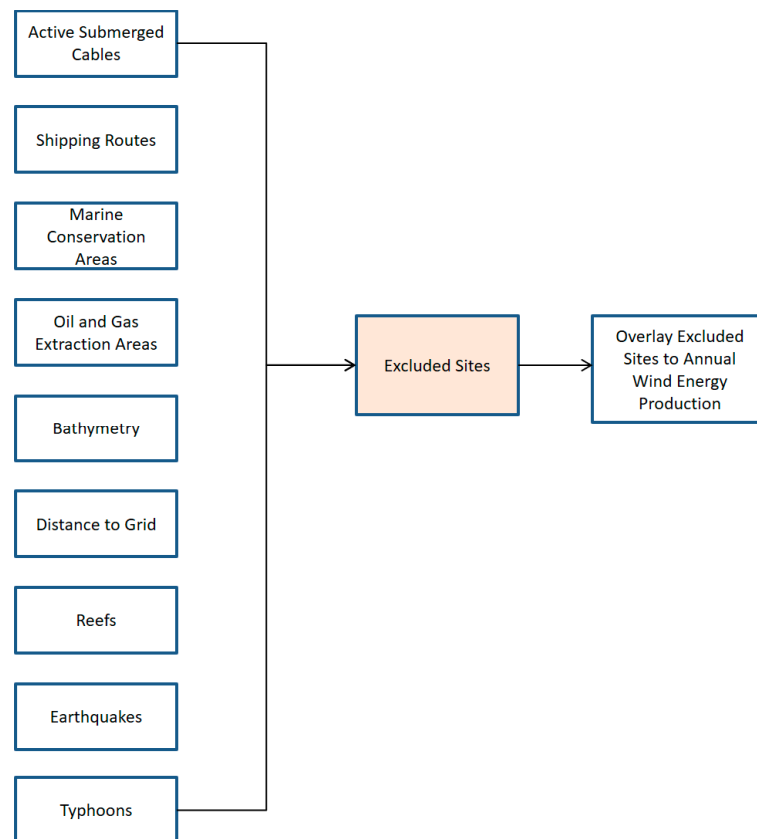


Figure 2. Detailed exclusion analysis.

Active submerged cable data were extracted from TeleGeography, and the map was projected to WGS 1984 UTM Zone 51 N, which is the projection for the Philippines. As seen in Figure 3, most of the active submerged cable is connected to the west part of Luzon near the capital of the Philippines—Manila City. This city is one of the most heavily populated areas and the center for business in the country, which explains the concentration of active submerged cables in the area. Luzon has the most active submerged cable connections that are connected from other countries, while Visayas and Mindanao are connected to Luzon for the interconnection of subsea cables. A buffer spacing of 5 km from the cables was applied for a conservative estimate that the offshore wind farm will not affect these cables.

Local ferry routes were extracted from the World Food Program. The map was projected to WGS 1984 UTM Zone 51 N, as shown in Figure 4. The path of the ferry routes in the Philippines all pass through the Visayas. Since the Philippines is composed of many islands, ferry routes are sometimes the only way to get to the other islands. The buffer spacing for the shipping route was 3 km, which is a conservative estimate considering an array spacing of 0.79 km² for a 126 m 6.2M126 turbine.

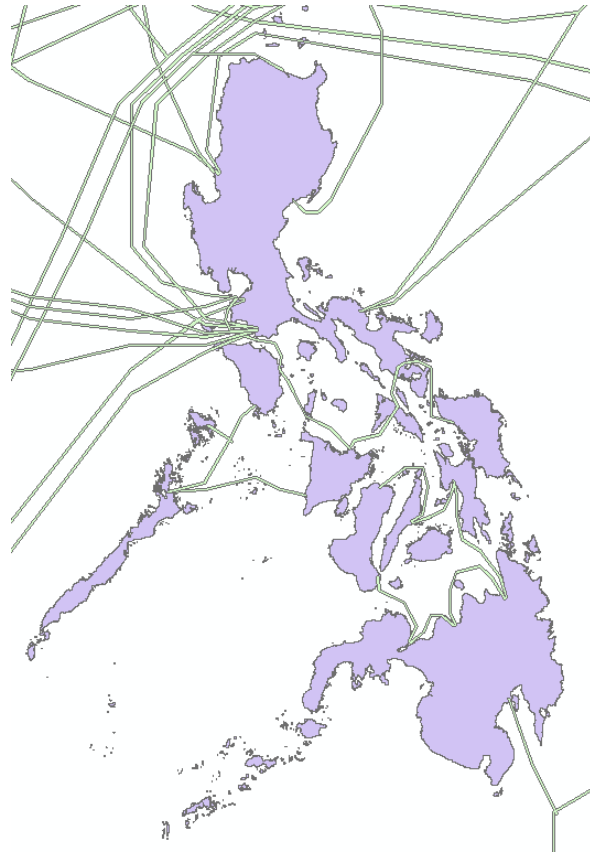


Figure 3. Active submerged cables.

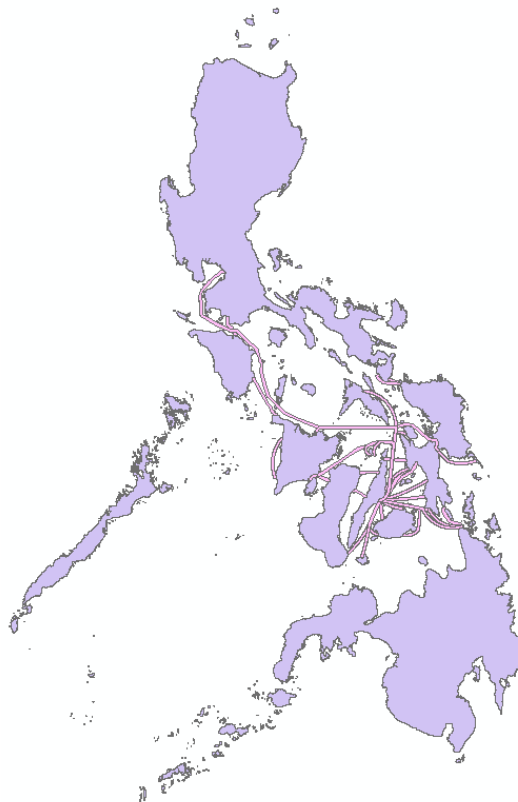


Figure 4. Local ferry routes.

The data for marine conservation areas were acquired from Protected Planet, which has an online world database of marine and terrestrial protected areas around the world. The data were used to generate a map using Arc GIS 10 with a projection of WGS 1984 UTM Zone 51 N, as shown in Figure 5. The map shows the nature reserve, natural park, natural monument, wildlife sanctuary, protected landscapes and seascapes, resource reserve, and natural biotic areas of the Philippines. Some of the evident marine protected areas in the map are the Tubbataha Reef, Turtle Islands Wildlife Sanctuary, Sarangani Bay, Siargao Protected Seascape, and Tanon Protected Seascape, Negros Occidental Coastal Wetlands Conservation Area, and Malampaya Sound. These marine protected areas were consolidated with other exclusion criteria to narrow down the potential location of the viability of offshore wind farms. The buffer spacing applied to the marine protected areas was 3 km, as already represented in the map.

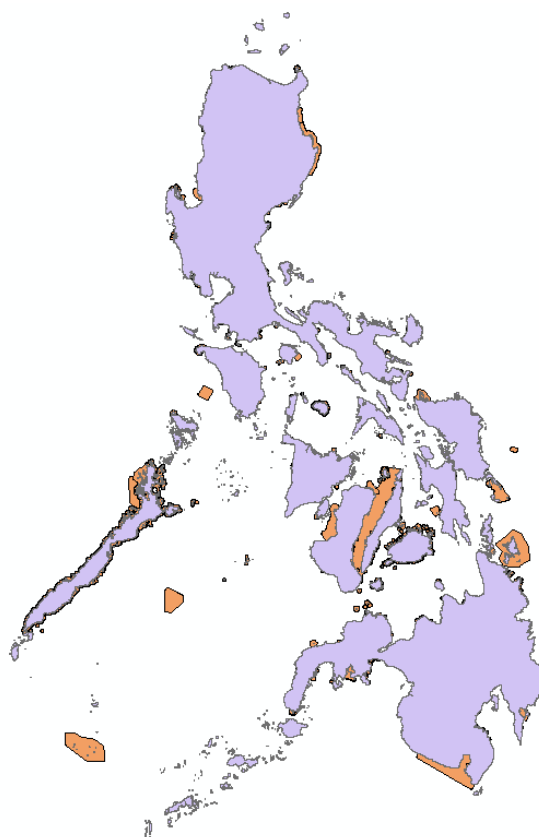


Figure 5. Marine conservation areas.

Coral reefs data in the Philippines were acquired from PhilGIS, which is a free GIS data source for educational and nonprofit use, and the reef data were from ReefBase, which is a global database for coral reefs. The data for reef were generated in a map using Arc GIS 10 with a projection of WGS 1984 UTM Zone 51 N, as shown in Figure 6. The types of reefs shown in the map are barrier, fringing, patch, and shelf reefs. The concentration of reefs is dominant in Visayas compared in Luzon and Mindanao. Similar to the marine protected areas, a buffer spacing of 3 km was applied in the exclusion of coral reefs.

Oil and gas extraction areas were acquired from the Department of Energy of the Philippines, and the map generated from Arc GIS was projected to WGS 1984 UTM Zone 51 N, as seen in Figure 7. The largest oil and gas extraction exploration in the Philippines is found at the east side of the Palawan Islands, which measures up to 1,476,000 km², and is headed by the Philippine National Oil Company (PNOC). Some of the other companies exploring oil and gas in the country are China International Mining Petroleum Corporation (197,000 km²), Mindoro-Palawan Oil and Gas Inc. (724,000 km²), Nido Petroleum

Philippines Pty. Ltd. (1,344,000 km²), PNOC (36,000 km²), Gas2Grid Ltd. (75,000 km²), Polyard Petroleum International Company (684,000 km²), Nido Petroleum Philippines Pty. Ltd. (314,000 km²), and Otto Energy Investments Ltd. (988,000 km²). These oil and gas exploration areas were consolidated with other exclusion criteria to narrow down the potential location of the viability of offshore wind farms. The buffer spacing considered for this criterion was 5 km, as shown in the map, so that the offshore wind farm will not affect the oil and gas extraction areas.

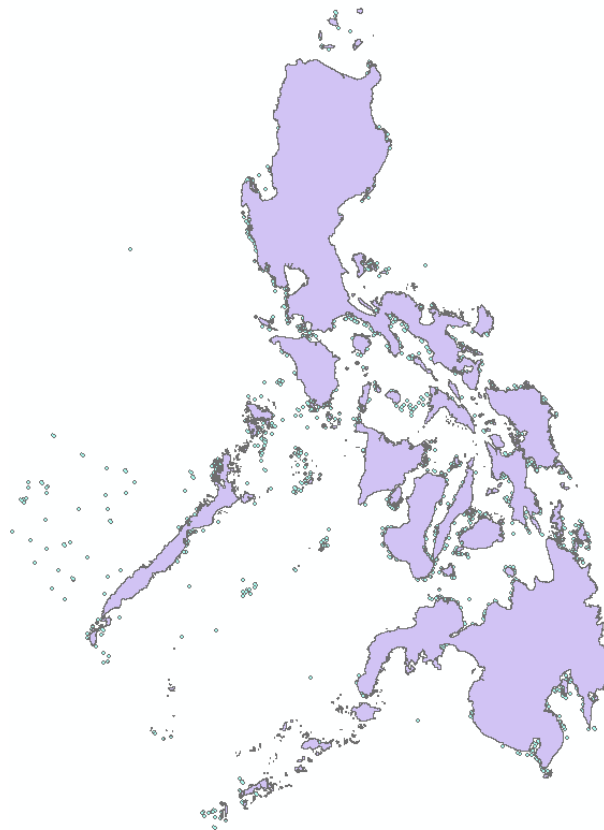


Figure 6. Coral reefs.

Bathymetry of the Philippines was acquired from the General Bathymetric Chart of the Oceans (GEBCO), and the map generated from Arc GIS was projected to WGS 1984 UTM Zone 51 N, as seen in Figure 8. The Reclassify tool in Arc GIS was used to remove the bathymetry greater than 50 m. The yellow areas represent the areas that were within the 50 m criteria. Areas greater than 50 m bathymetry were excluded in the analysis together with other exclusion criteria to narrow down the potential location of the viability of offshore wind farms.

The data from the National Renewable Energy data explorer on the grid of the Philippines were used in this study, and the map generated using Arc GIS was projected to WGS 1984 UTM Zone 51 N, as seen in Figure 9. The Euclidean Distance tool was used to generate a map with the corresponding distance from the grid. The Reclassify tool was then used to remove the values greater than 120 km distance from the grid. Areas beyond 120 km or outside of the green shade in the map were excluded in the analysis. The distance greater than 120 km and other exclusion criteria were consolidated to narrow down the potential sites for the analysis.

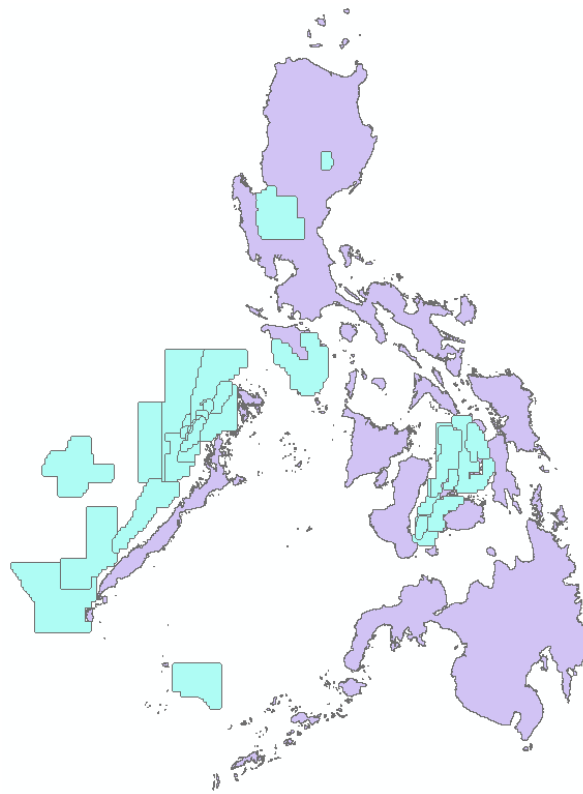


Figure 7. Oil and gas extraction areas.

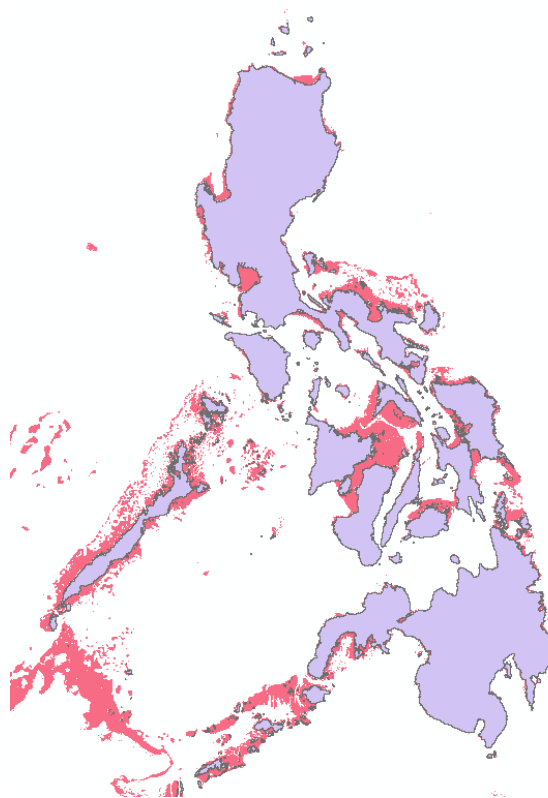


Figure 8. Bathymetry within 50 m.

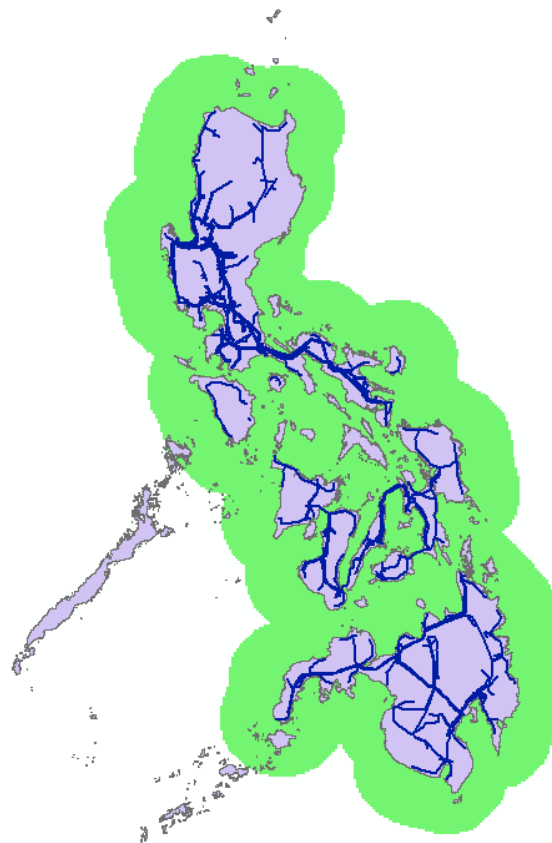


Figure 9. Distance to grid within 120 km.

Historical earthquakes were acquired from the Philippine Institute of Volcanology and Seismology (PHIVOLCS). The acquired data were composed of the recorded magnitude and location of earthquakes in the Philippines from 1908 to 2018. The earthquakes with 6.5 magnitude and above were plotted in Arc GIS with a projection of WGS 1984 UTM Zone 51 N, as seen in Figure 10. A buffer area of 15 km was applied to the study area based on the critical damage extent to a dyke of a 7.8 magnitude earthquake in Japan [40].

The typhoon path and wind speed data of the Philippines were acquired from the Philippine Atmospheric Geophysical and Astronomical Services Administration (PAGASA). The gathered data spans from 1998 to 2018. The map was generated using Arc GIS with a projection of WGS 1984 UTM Zone 51 N, as illustrated in Figure 11. The highest historical typhoon that landed in the Philippines is Typhoon Yolanda (International Name: Haiyan), with a wind speed reaching 315 km/h (indicated by the red path). The path considered were those typhoons that reached greater than 250 km/h from 1998 to 2018. A buffer area of 50 km was applied in the exclusion of historical typhoon paths.

A graph digitizer was used to produce the power curve of SWT-3.6-120 and 6.2M126, as seen in Figures 12 and 13, respectively. A total of 562 and 270 data points were plotted based on the power curve of the SWT-3.6-120 brochure and power curve of 6.2M126, respectively. The x -axis represents the wind speed in m/s, and the y -axis represents the power output in kW of the wind turbine.

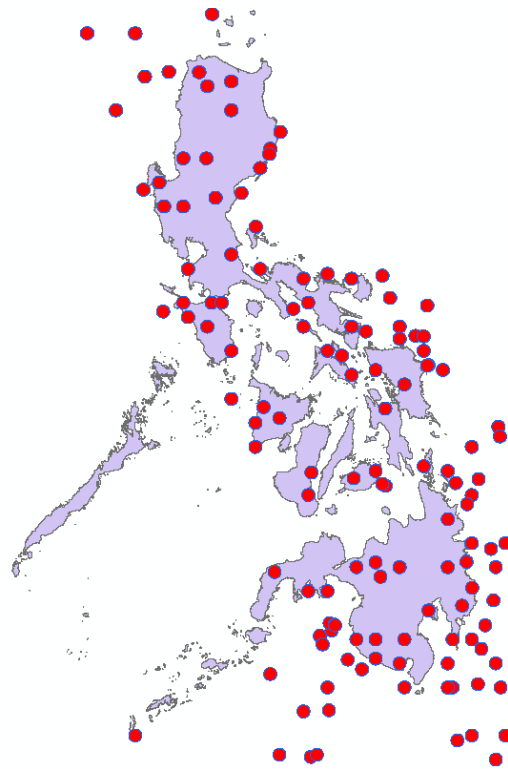


Figure 10. Earthquakes with at least a 6.5 magnitude.

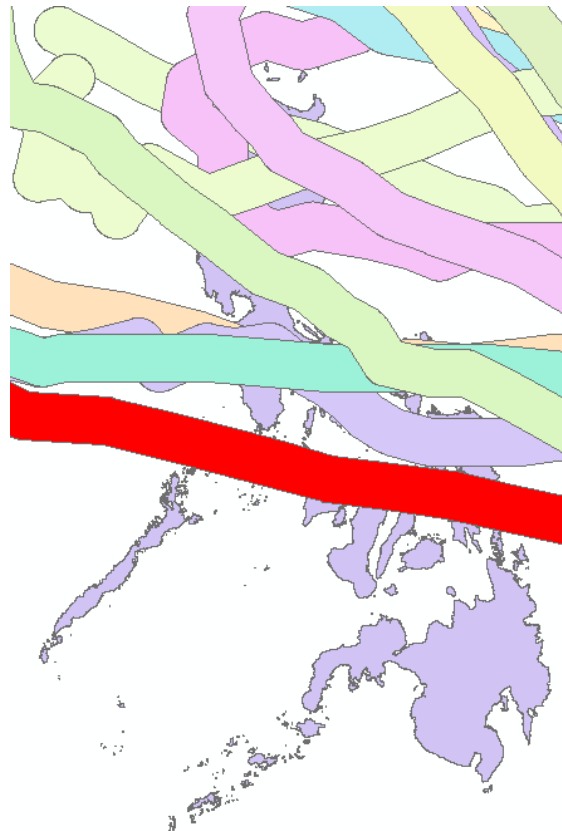


Figure 11. Typhoons with greater than 250 km/h.

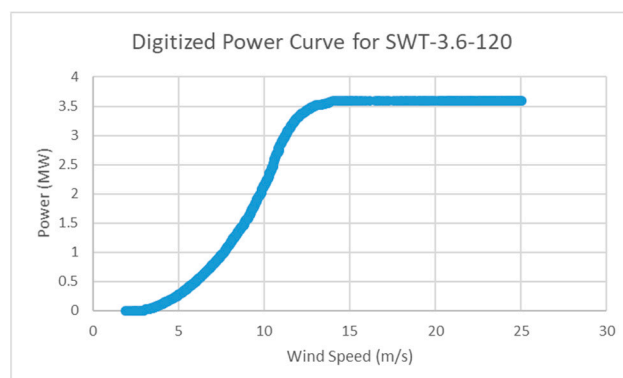


Figure 12. Power curve of Siemens SWT-3.6-120.

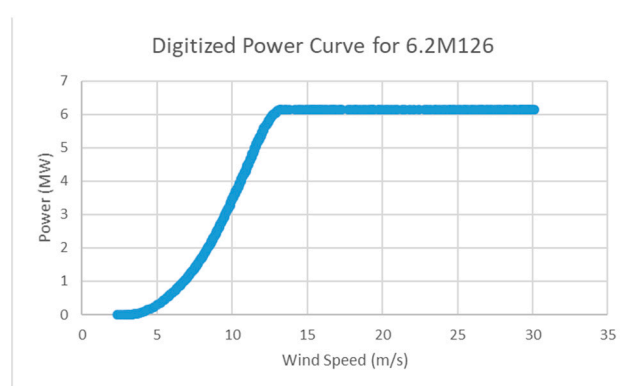


Figure 13. Power curve of Senvion 6.2M126.

3.1.2. Technical Analysis

The detailed technical analysis can be seen in Figure 14. The acquired wind speed data were at 80 m and necessitated being extrapolated to the hub height of SWT-3.6-120 at 90 m and hub height of 6.2M126 at 95 m using the Power Law in Equation (1). Equation (3) allows for the computation of the wind power density and wind power utilizing the Weibull function model of SWT-3.6-120 and 6.2M126. To compute the annual wind energy production, the power curve of the selected turbines and their corresponding Weibull functions were used as inputs to Equation (4). Capacity factor and performance were computed using Equations (5) and (6), respectively. After generating the annual capacity factor and performance maps, the exclusion criteria layer was masked over to remove the unsuitable locations from the potential sites for OWF and the investment cost from the regression model was applied to calculate the levelized cost of electricity and offshore wind electricity price in the Philippines. Finally, the two turbines were then compared with the *LCOE* at different areas and plant capacities.

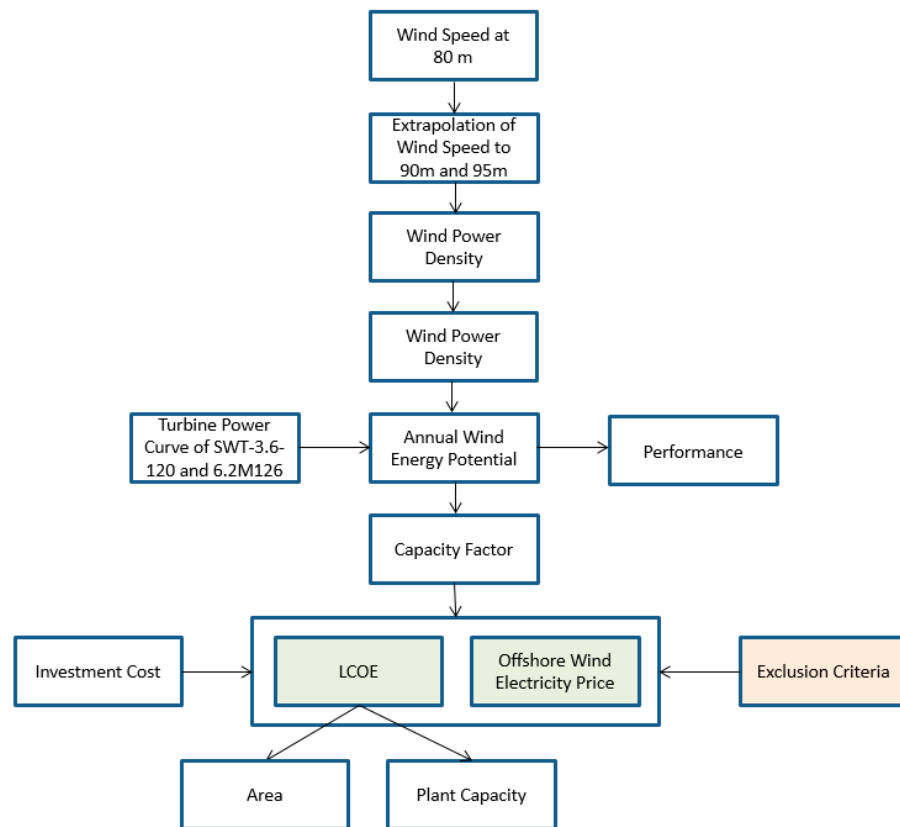


Figure 14. Detailed technical analysis.

3.1.3. Economic Analysis

The detailed economic analysis of the study can be seen in Figure 15. The independent variables considered for the electrical cost of offshore wind farms were onshore cable length, offshore cable length, inter-array cable length, and the area. For the turbine cost, the plant capacity was the considered independent variable in the analysis. The selection of these variables were based on the premise that the cables are the major components of the electrical cost and that the turbine cost is dependent on the plant capacity [17,20,51]. The independent variables for the foundation cost depend on the bathymetry of the ocean and the size of the turbine [59]. The nearest port distance was considered for the maintenance and operation [20,59].

The data for independent variables were acquired from “4COffshore”, which is a market research and consultancy organization that focuses on offshore energy markets, and it has been cited in numerous studies [51–53]. The data acquired were name of power plant, country of origin, minimum and maximum sea depth, area, offshore cable length, onshore cable length, inter-array cable length, port for O&M, distance from port, turbine model, number of turbines, turbine capacity, plant capacity, and investment cost. All the values for investment cost in different years were converted to 2017 USD using the historical values of each country and the historical USD exchange rate. The nearest port distances were acquired based on the visual inspection in the 4COffshore wind map, and the distance between the nearest port and offshore wind farm was measured through the difference of their coordinates. The missing onshore cable length was estimated based on the location of the stated grid connection point and the cable landing point through the difference of their coordinates. The four regression assumptions were checked using the R statistical software. The “lm” function was used to generate the multiple linear regression model. The “plot” function was used to test the normality, linearity, homoscedasticity, and reliability of the model with the visual inspection of the normal Q–Q plot, residual vs. fitted plot, scale-location plot, and residual vs. leverage plot, respectively. The reliability of the model was

further examined using the “vif” function, which determines the independent variables with multicollinearity. The independent variables with vif greater than 10 were carefully omitted. The selected regression model was validated using actual data from offshore wind farms through the measure of mean absolute percentage error. The investment cost calculated using the selected regression model was applied together with the capacity factor and exclusion criteria to acquire the *LCOE* and offshore wind electricity price in the Philippines.

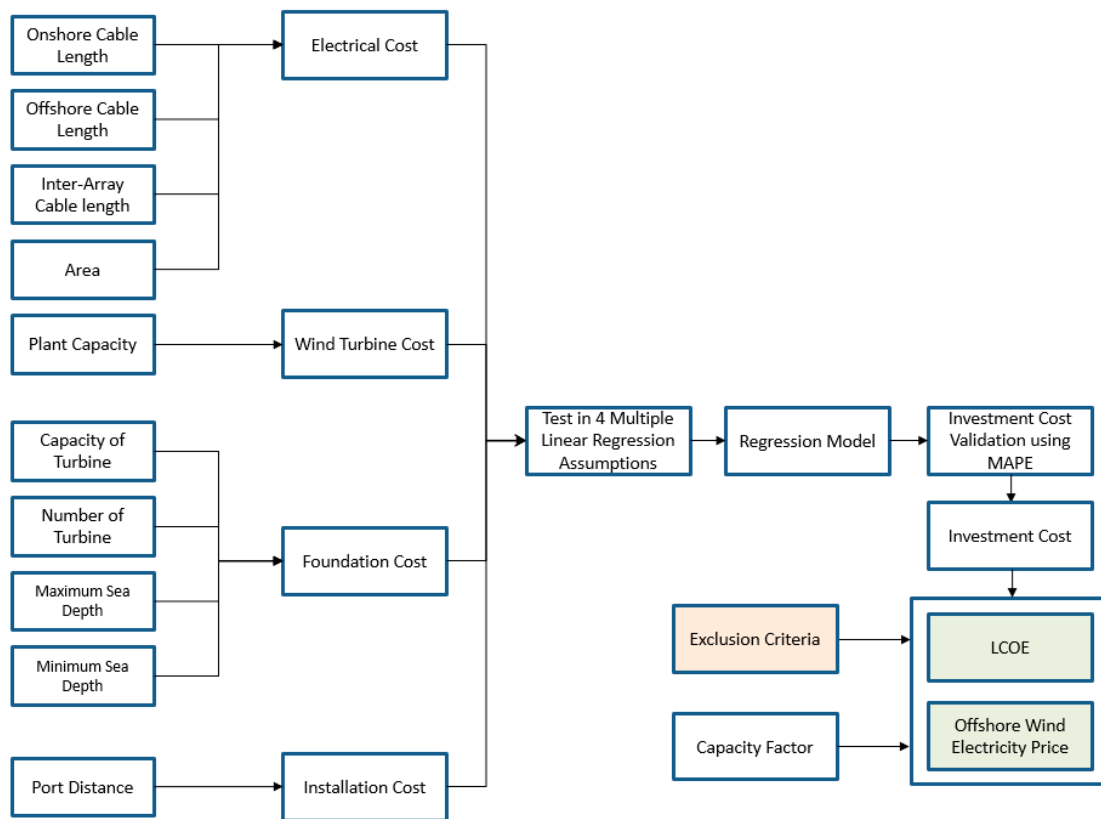


Figure 15. Detailed economic analysis.

3.1.4. Sensitivity Analysis

Sensitivity analysis was carried out in the last part of the study to determine the effect of certain parameters to the output values under a given set of assumptions. The parameters that were analyzed to check the sensitivity to the resulting *LCOE* and price of electricity were investment cost (\pm mean absolute percentage error), capacity factor ($\pm 2\%$), weighted average cost of capital ($\pm 2\%$), cost of debt ($\pm 1\%$), cost of equity ($\pm 2\%$), and plant capacity ($\pm 5\%$). The basis in the adjustment of the parameters were small reasonable changes based on the nature of the parameters.

3.2. R Statistical Software

The R statistical software was used for handling the 128,000 by 26 data points for the technical analysis. A program was also implemented to calculate the wind speed at 90 m, Weibull probability density function, wind power density, wind power, annual energy production, capacity factor, and performance. The statistical tools of R were used to acquire the equation for the multiple linear regression in the economic analysis.

3.3. GIS Software

Geospatial information system (GIS) methodology has been widely used by different researchers in describing the technical and economic potential of offshore wind farms. It

is a modeling tool that can relate the costs, location, and power plant capacity through displayed resources, spatial cost, and restrictions in areas. The main product of this is the relation of the levelized cost of electricity (LCOE) to the spatial area of study [17].

The Arc GIS 10 software requires the wind speed data resource in the location of study, bathymetry, cable distance as well as the economic factors involved in the construction of an offshore wind farm. This modeling tool can compute for various cost algorithms to get the LCOE [20].

4. Results and Discussions

4.1. Technical Analysis

The recommended hub heights for the Siemens SWT-3.6-120 and Senvion 6.2M126 were 90 m and 95 m, respectively. As such, the wind speed data at 80 m were extrapolated to these two elevations. The succeeding analysis will show the technical parameters corresponding to both turbines plotted in their ideal elevations.

4.1.1. Wind Speed

The data on wind speed at 80 m were extrapolated to a hub height of 90 m for the SWT-3.6-120 and to 95 m for the Senvion 6.2M126 using the power law in Equation (1). Figure 16a,b shows the average wind speeds of the Philippines for the SWT-3.6-120 and 6.2M126, respectively, from the years 2008, 2010, 2014, 2015, and 2016.

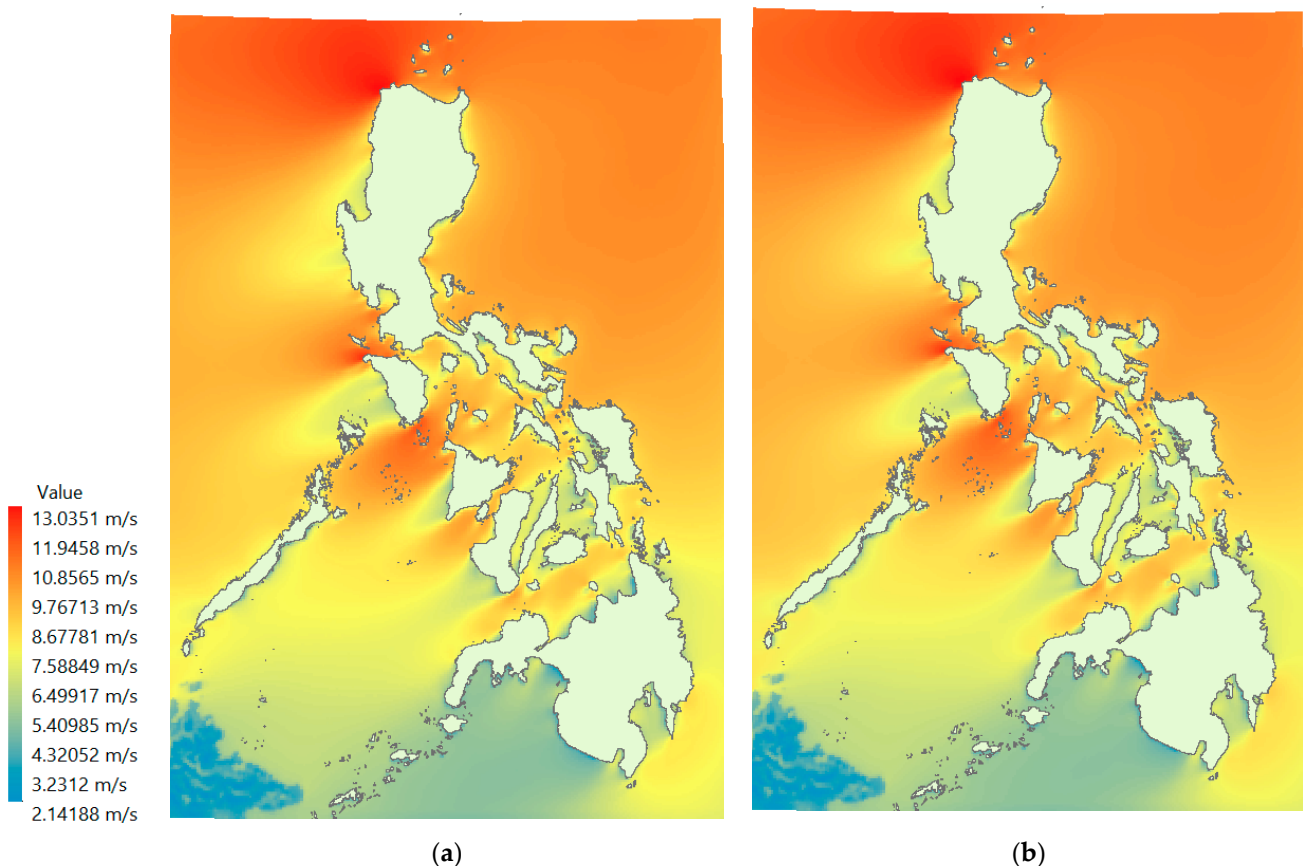


Figure 16. Wind speed at a hub height of (a) SWT-3.6-120 and (b) 6.2M126.

Shown in Figure 16a is the contour plot of wind speed for the Siemens SWT-3.6-120 turbine hub height. The values range from 2.133 m/s to 12.981 m/s with an average of 8.041 m/s. The northern parts of Ilocos Norte sees the greatest wind speeds ranging from 10.611 m/s to 12.945 m/s. Coming in next are the northern parts of Occidental Mindoro and the southeastern parts of Oriental Mindoro, which see wind speed values from 9.175 m/s

to 12.091 m/s and from 9.091 m/s to 11.63 m/s, respectively. Luzon primarily sees greater wind speeds than Visayas and most especially Mindanao, as evidenced in the blue contours indicating lower values shown in the regions of the latter island.

For the Senvion 6.2M126 hub height, wind speeds vary from 2.142 m/s to 13.035 m/s with a mean of 8.096 m/s. The contours are shown in Figure 16b. As expected, the wind speed values seen by the Senvion turbine were higher than those of the Siemens case due to a slightly higher elevation. Additionally expected were the locations of greatest wind speeds since the extrapolation will result in the same trends due to a common roughness factor for all offshore areas studied. The northern region of Ilocos Norte experiences wind speeds of 10.655 m/s up to 12.991 m/s while the northern region of Occidental Mindoro sees 9.213 m/s to 12.325 m/s speeds, and the southeastern region of Oriental Mindoro experience speeds from 9.279 m/s to 11.678 m/s.

4.1.2. Wind Power Density

The average wind power density for SWT-3.6-120 and 6.2M126 in the years 2008, 2010, 2014, 2015, and 2016 can be seen in Figure 17a,b. It is worth noting that the mean wind power density is independent of the turbine, and is the power density of the wind for the area. For the wind power density of SWT-3.6-120, the lowest was at 11.539 W/m² and the highest was at 1777.830 W/m², as seen in Figure 17a. The mean of the wind power density was at 700.918 W/m². Corresponding to the areas of greatest wind speeds were those of the greatest wind power densities with the northern region of Ilocos Norte ranging from 1238.358 W/m² to 1771.519 W/m², the northern region of Occidental Mindoro seeing 882.755 W/m² to 1604.634 W/m², and finally, the southeastern region of Oriental Mindoro ranging from 873.324 W/m² to 1499.410 W/m². For the wind power density of 6.2M126, the lowest was at 11.683 W/m² and the highest was at 2257.367 W/m², as seen in Figure 17b. The mean of the wind power density was at 753.835 W/m². Compared with SWT-3.6-120, there were increases of 1.25%, 26.97%, and 7.55% in the lowest, highest, and mean wind power densities, respectively. There was a variation in the increase of these measures due to the nature of the equation, which is dependent on the cube of the wind speed and the different Weibull probability distribution model for each turbine. The wind Weibull probability distribution model for SWT-3.6-120 takes into account 26 integers from 0 to 25, which represents the wind speed it operates in, while the 6.2M126 model takes into account 31 integers from 0 to 30. Similar to the results of SWT-3.6-120, the locations with the greatest wind power densities (as shown in the red contours) were found in the northern parts of Ilocos Norte, which had values ranging from 1405.655 W/m² to 2241.579 W/m² while the northern parts of Occidental Mindoro and the southeastern parts of Oriental Mindoro experience densities ranging from 937.934 W/m² to 1999.059 W/m² and 955.461 W/m² to 1757.770 W/m², respectively.

4.1.3. Wind Power

The average annual wind power for the Siemens SWT-3.6-120 and Senvion 6.2M126 are presented in Figure 18a,b. Wind power is a function of the diameter of the rotor (see Equation (3)). The Siemens SWT-3.6-120 has a diameter of 120 m while the Senvion 6.2M126 has a diameter of 126. One can surmise that the Senvion should produce greater wind power due to greater wind speeds as well as a greater swept area.

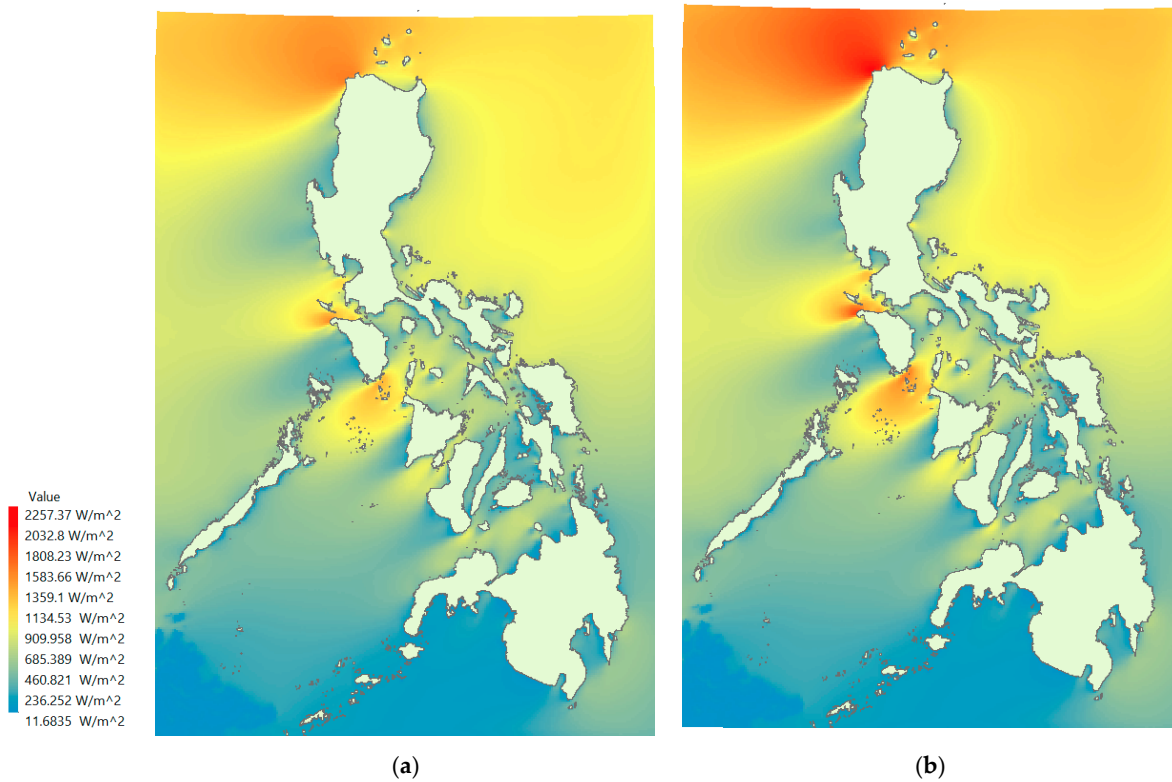


Figure 17. Wind power density for (a) SWT-3.6-120 and (b) 6.2M126.

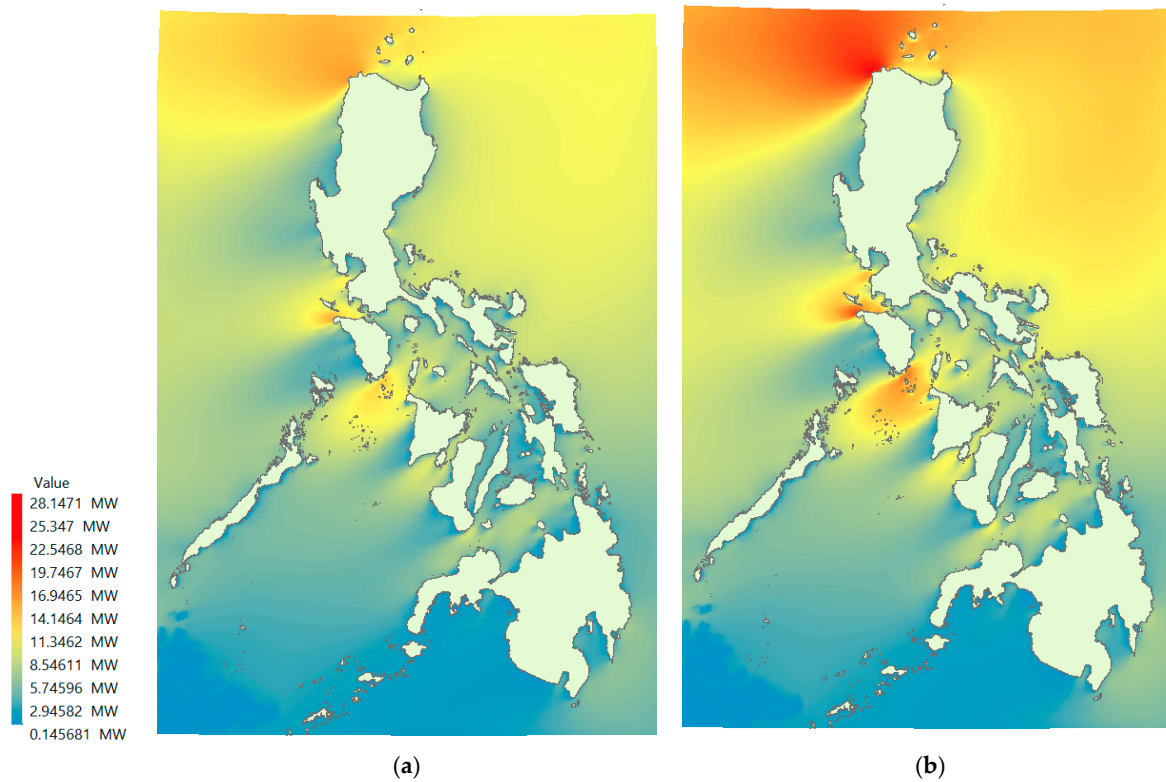


Figure 18. Wind power for (a) SWT-3.6-120 and (b) 6.2M126.

In studying SWT-3.6-120, the least wind power observed was 0.131 MW, while the greatest was 20.107 MW. The mean wind power observed was 7.927 MW. As with the wind

power density, the locations that registered the greatest wind power were the ones in the northern region of Ilocos Norte, reaching low values of 14.006 MW and high values of 20.035 MW. Furthermore, the northern region of Occidental Mindoro and the southeastern region of Oriental Mindoro register wind power ranges from 9.984 MW to 18.148 MW and from 9.877 MW to 16.958 MW, respectively, and seen as orange contours in the map. Using the same analysis for Senvion 6.2M126, the least value of wind power observed was 0.146 MW while the greatest value was 28.147 MW, with the latter clearly seen in Figure 18b. The average annual wind power was 9.4 MW. Compared to the Siemens rotor, one can observe an increase in the power metrics for the Senvion case with a computed 11.45%, 39.99%, and 18.58% increase in the least, greatest, and average wind power, respectively. The wind Weibull probability distribution model for SWT-3.6-120 takes into account 26 integers from 0 to 25, which represents the operational wind speed, while the 6.2M126 model takes into account 31 integers from 0 to 30. Consistent with the previous results, the greatest wind power densities were located in the northern regions of Ilocos Norte with power values ranging from 17.527 MW to 27.950 MW. Following suit were the areas in the northern regions of Occidental Mindoro and the southeastern regions of Oriental Mindoro, registering values of 11.695 MW to 24.926 MW and 11.914 MW to 21.918 MW, respectively.

4.1.4. Annual Energy Production

Shown in Figure 19a,b are the mean annual energy production for both turbines studied. The Siemens SWT-3.6-120 produces at least 179.519 MWh and at most 19,759.275 MWh. The average annual energy production is 11,905.933 MWh. As expected, one can find the highest potential in the same locations as those of the greatest wind speed and wind power recorded. These are the northern parts of Ilocos Norte, producing 17,181.576 MWh to 19,742.881 MWh of energy per year. Likewise, the northern parts of Occidental Mindoro produced high yields at 14,763.450 MWh to 19,212.203 MWh whereas the southeastern parts of Oriental Mindoro produced around 14,379.013 MWh to 18,769.434 MWh of energy. Areas with low energy production were observed close to the shorelines of Visayas and Mindanao.

The analysis further showed that the Senvion 6.2M126 produced the least energy at a rate of 155.305 MWh and the greatest at 34,974.594 MWh. The contours of annual energy production are shown in Figure 19b. The average energy produced was 19,550.665 MWh. While there were increases in the mean and greatest energy production versus the Siemens turbine at 77% and 64.21%, respectively, a drop of 13.49% was observed in the lowest energy production. This drop was likely due to a higher cut-in wind speed of the Senvion 6.2M126 which is at 3.5 m/s. Despite the higher cut-in wind speed, the Senvion makes up in energy production as the greatest production rate and mean production rate were both significantly higher than that of the Siemens. At a higher rated capacity of 6.15 MW and higher wind speed seen, the Senvion naturally outperformed the Siemens in energy production. The sites with the greatest production of energy were in the same locations as those of wind speed and wind power. The northern areas of Ilocos Norte can potentially produce energy from 29,111.229 MWh to 34,903.898 MWh with the northern areas of Occidental Mindoro and southeastern areas of Oriental Mindoro producing 24,404.434 MWh to 33,724.617 MWh and 24,664.807 MWh to 32,284.715 MWh, respectively.

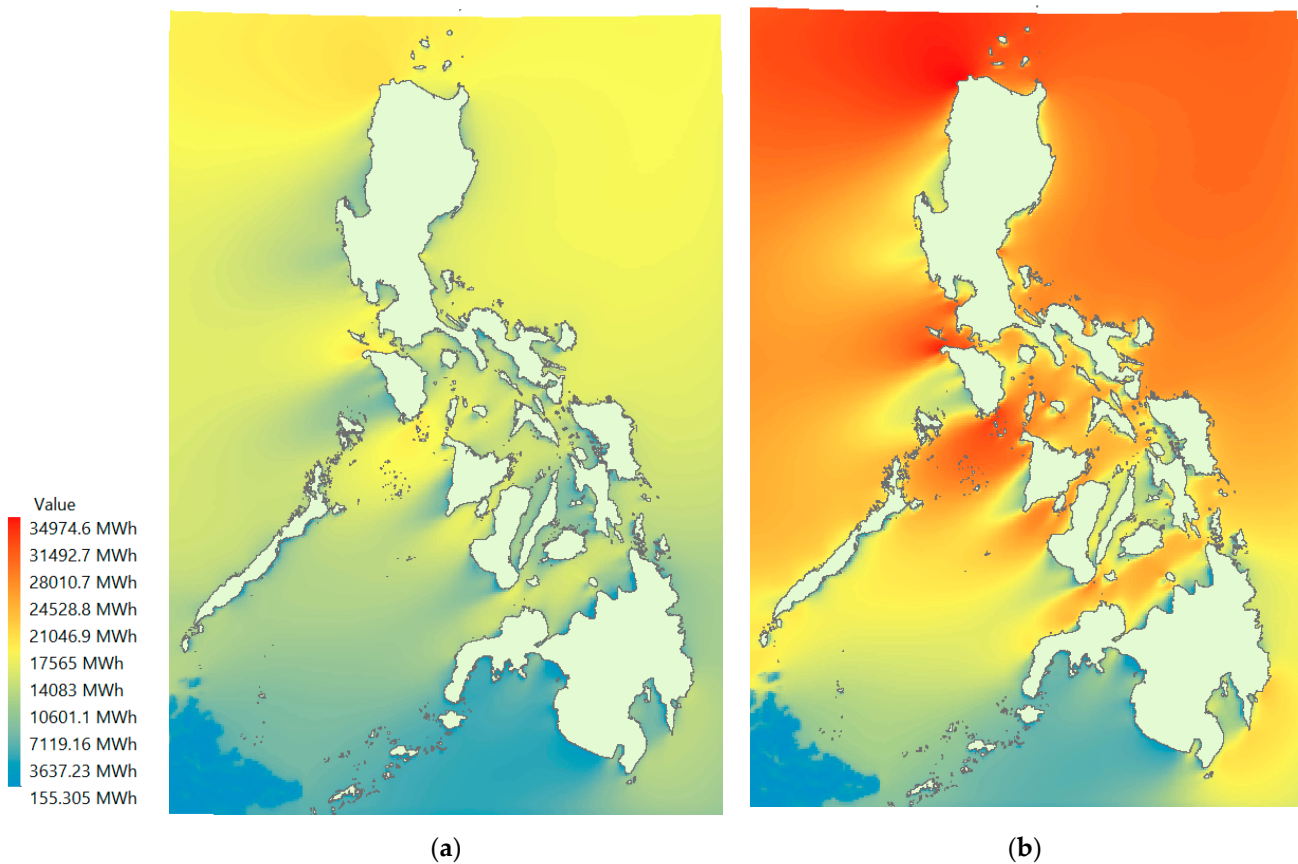


Figure 19. Annual energy production of (a) SWT-3.6-120 and (b) 6.2M126.

4.1.5. Capacity Factor

Shown in Figure 20a,b are the computed capacity factors of the Siemens SWT-3.6-120 and the Senvion 6.2M126, respectively. The red contours indicate high capacity factor, while the blue contours indicate low capacity factor. The lowest, mean, and highest capacity factors computed for the Siemens SWT-3.6-120 were 0.57%, 37.75%, and 62.66%, respectively. Very high values of 54.48% to 62.60% were observed in the northern parts of Ilocos Norte. Similarly, high values were also seen around the northern parts of Occidental Mindoro ranging from 46.81% to 60.92% as well as the southeastern parts of Oriental Mindoro ranging from 45.60% to 59.52%.

The lowest, mean, and highest capacity factors computed for the Senvion 6.2M126 were 0.29%, 36.29%, and 64.92%, respectively. In the same manner that the lowest value of annual energy production was significantly lower than that of the Siemens turbine, the least capacity factor was recorded to have dropped by 49.12%. There was also a decrease in the mean capacity factor by 3.87%, while an increase in the greatest capacity factor value by 3.6% was observed. The top three areas with the greatest capacity factors were the northern region of Ilocos Norte registering values from 54.04% to 64.79%, the northern region of Occidental Mindoro with recorded values of 45.30% to 62.60%, and the southeastern region of Oriental Mindoro reaching a range of 45.78% to 59.93%. Figure 21a,b show the capacity factor with less than 30% for SWT-3.6-120 and 6.2M126, respectively, indicated by the black contours. In this study, areas that had a capacity factor less than 30% were excluded in the potential siting of offshore wind farms.

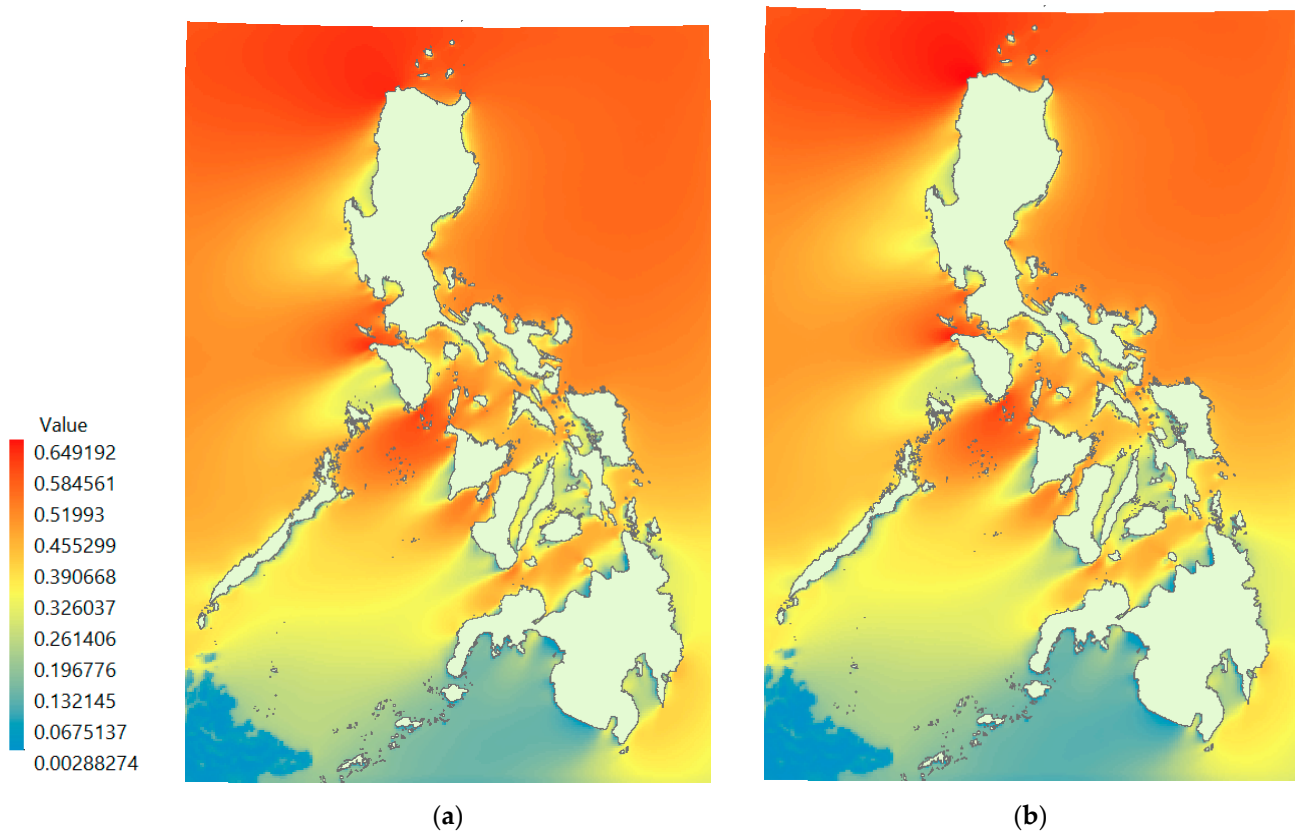


Figure 20. Capacity factor of (a) SWT-3.6-120 and (b) 6.2M126.

4.1.6. Performance

The performance and the ratio between the energy produced by the wind turbine and the wind energy available of the Siemens SWT-3.6-120 and the Senvion 6.2M126 are shown in Figure 22a,b. The worst performance computed for the Siemens SWT-3.6-120 was 11.27%, while the recorded best performance was 29.89%. On average, the performance of the Siemens turbine was 20.60%. The poorest performing areas were the northern region of Ilocos Norte, the northern region of Occidental Mindoro, and the southeastern region of Oriental Mindoro, with performance ranging from 11.30% to 14.62%, 12.13% to 17.62%, and 12.70% to 18.17%, respectively. The contrasting results between performance and the previous parameters are not surprising since performance-wise, the two turbines are able to maximize the energy conversion available when the wind speeds are lower. At higher wind speeds that translate to higher wind power and capacity factor, the wind turbine conversion is limited to the capacity of the system and is fixed at its declared rating. This means that there is more energy in the wind that is not converted due to the limitation of the energy converter (flat line power output beyond the rated wind speed of about 13 m/s).

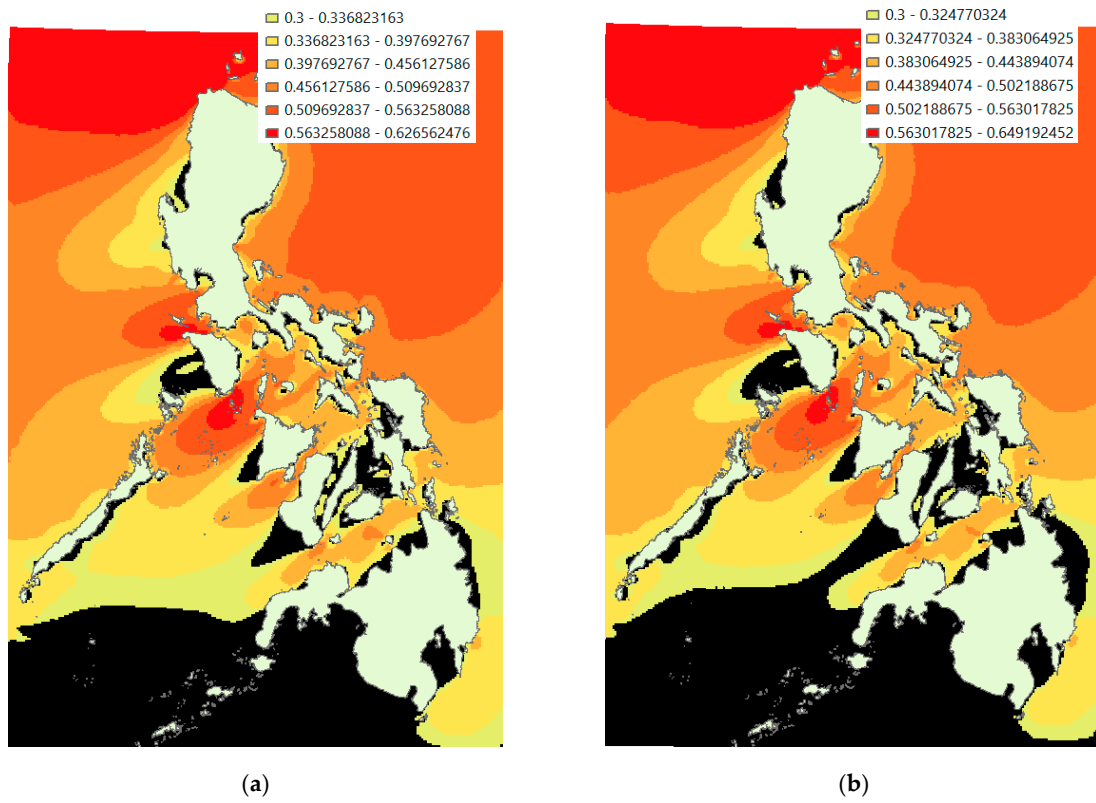


Figure 21. Black contours with less than 30% capacity factor for (a) SWT-3.6-120, (b) 6.2M126.

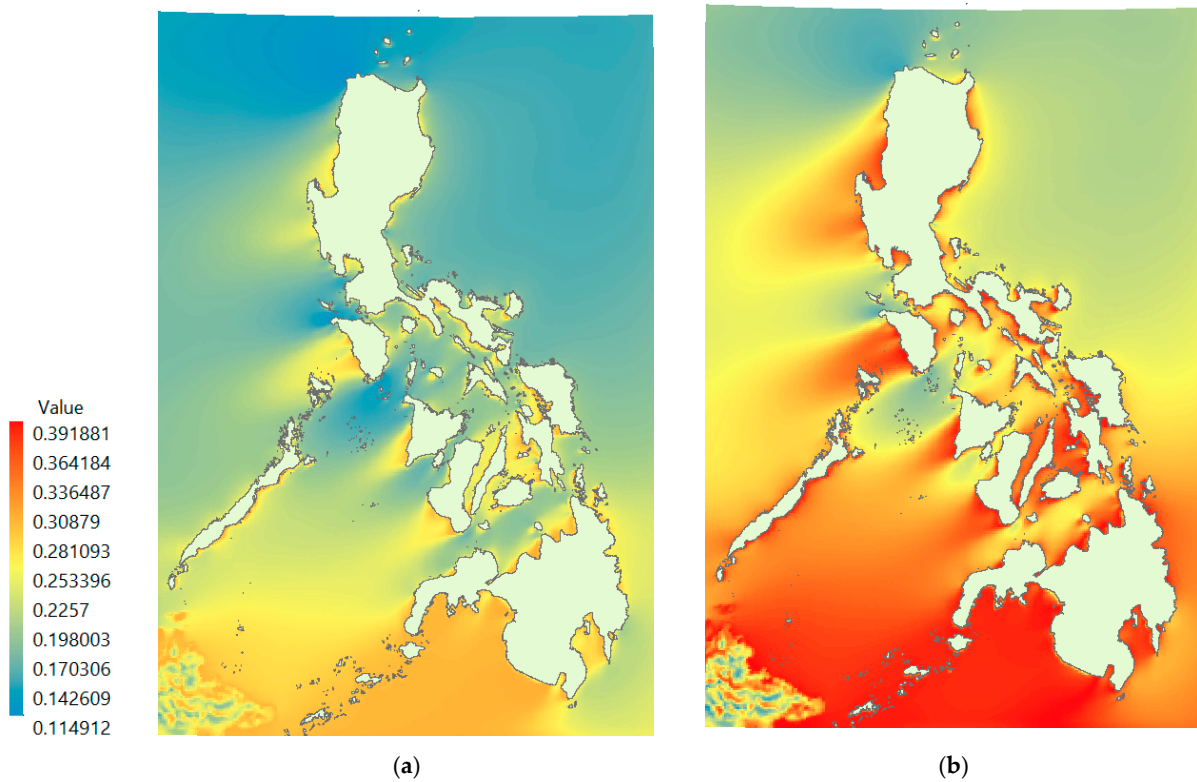


Figure 22. Performance of (a) SWT-3.6-120 and (b) 6.2M126.

The worst performance of the Senvion 6.2M126 was comparable to the Siemens turbine at 11.49%, while the best performance was recorded higher at 39.19%. The average

performance was also better than the Siemens at 28.26%. The improvement in performance relative to the Siemens turbine can be attributed to higher annual energy production. Probing the performance map, one can observe that the low performing regions correspond, unsurprisingly, to the areas of best wind power. These poorest performing areas were the northern parts of Ilocos Norte with rates ranging from 14.41% to 20.23%, the northern parts of Occidental Mindoro with figures of 15.89% to 25.14%, and the southeastern parts of Oriental Mindoro performed slightly better but were still very low at 16.97 to 24.85%. Again, the results revealed the inverse effect of high capacity factor to low performance since high wind power outbalances the influence of the annual energy production. Conversely, high performing areas usually have low values of capacity factor due to lower wind power values.

4.2. Application of Exclusion Criteria

Applying all exclusion criteria on the capacity factor layer, the sites that are potentially viable for deployment of wind farms for both wind turbines studied are shown in Figures 23 and 24. These locations are namely the (i) north of Cagayan, (ii) west of Rizal, (iii) north of Camarines Sur, (iv) north of Samar, (v) southwest of Masbate, (vi) Dinagat Island, (vii) Guimaras, and (viii) northeast of Palawan. These areas identified are shown in patches of green and dot the map all over the country from the north or Luzon to the northernmost tip of Mindanao. From the previous sections, one can make the conclusion that the top three areas would still be the same ones at the end of the analysis. Unfortunately, the three best areas were excluded after the exclusion mask was applied. The resulting map with the highest capacity factor shows the areas north of Luzon in the Cagayan region as the best for wind farm development. The Siemens SWT-3.6-120 capacity factor range was from 50.32% to 41.71% while the Senvion 6.2M126 capacity factor range was from 48.42% to 38.56%. This location was the same site used for the economic analysis.

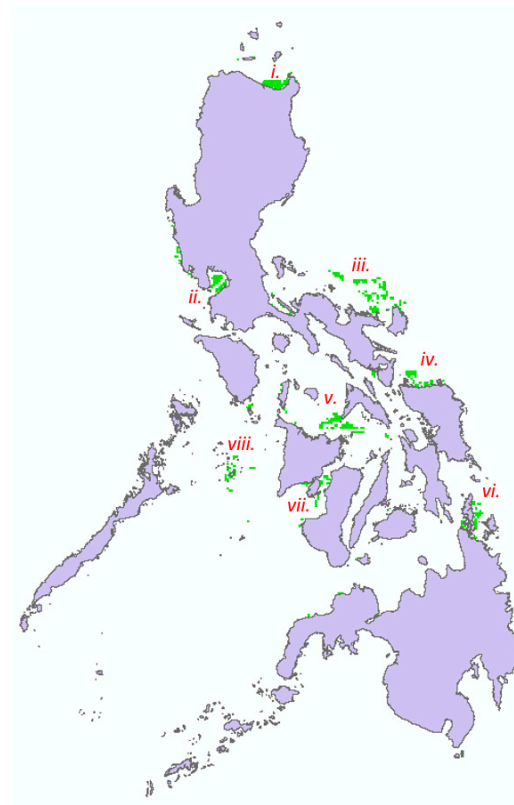


Figure 23. Offshore wind farms sites for SWT-3.6-120.

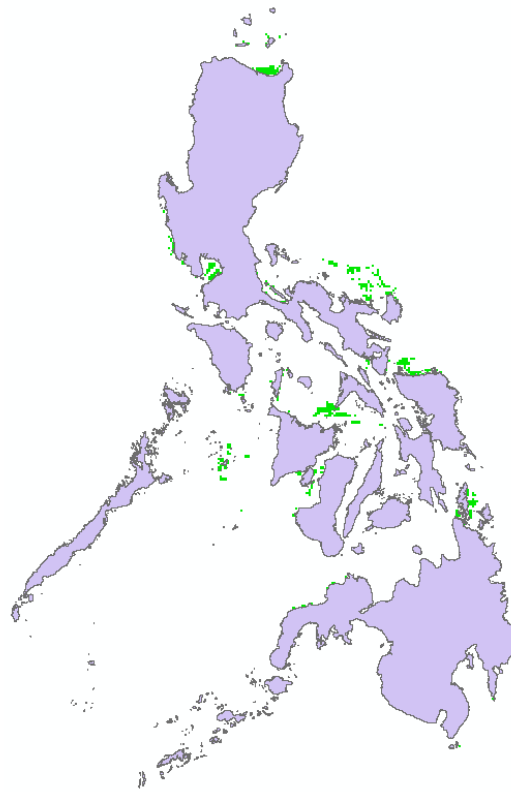


Figure 24. Offshore wind farms sites for 6.2M126.

4.3. Economic Analysis

4.3.1. Multiple Linear Regression

The data for independent variables were acquired from “4COffshore”. There were 63 observations acquired for the offshore wind farms with the corresponding name of power plant, country of origin, minimum and maximum sea depth, area, offshore cable length, onshore cable length, inter-array cable length, port for O&M, distance from port, turbine model, number of turbines, turbine capacity, plant capacity, and investment cost. The first 39 observations acquired were separated in a different spreadsheet that used the multiple linear regression model, while the other 24 observations were used for validation of the model generated.

4.3.2. Regression Model Diagnostics

Figure 25a–d illustrates the four-assumption test with the exclusion of three observations. The observations followed a normal distribution, as shown in Figure 25a. It also displayed linearity and homoscedasticity, as seen in Figure 25b,c, respectively. Finally, the reliability test through the residuals vs. leverage plot showed that there was no influential observation that was outside the trend. The next step in checking the assumptions of multiple linear regression is the variance inflation factor test, which indicates if there is multicollinearity between the independent variables. The three observations were omitted due to failure in satisfying the reliability test.

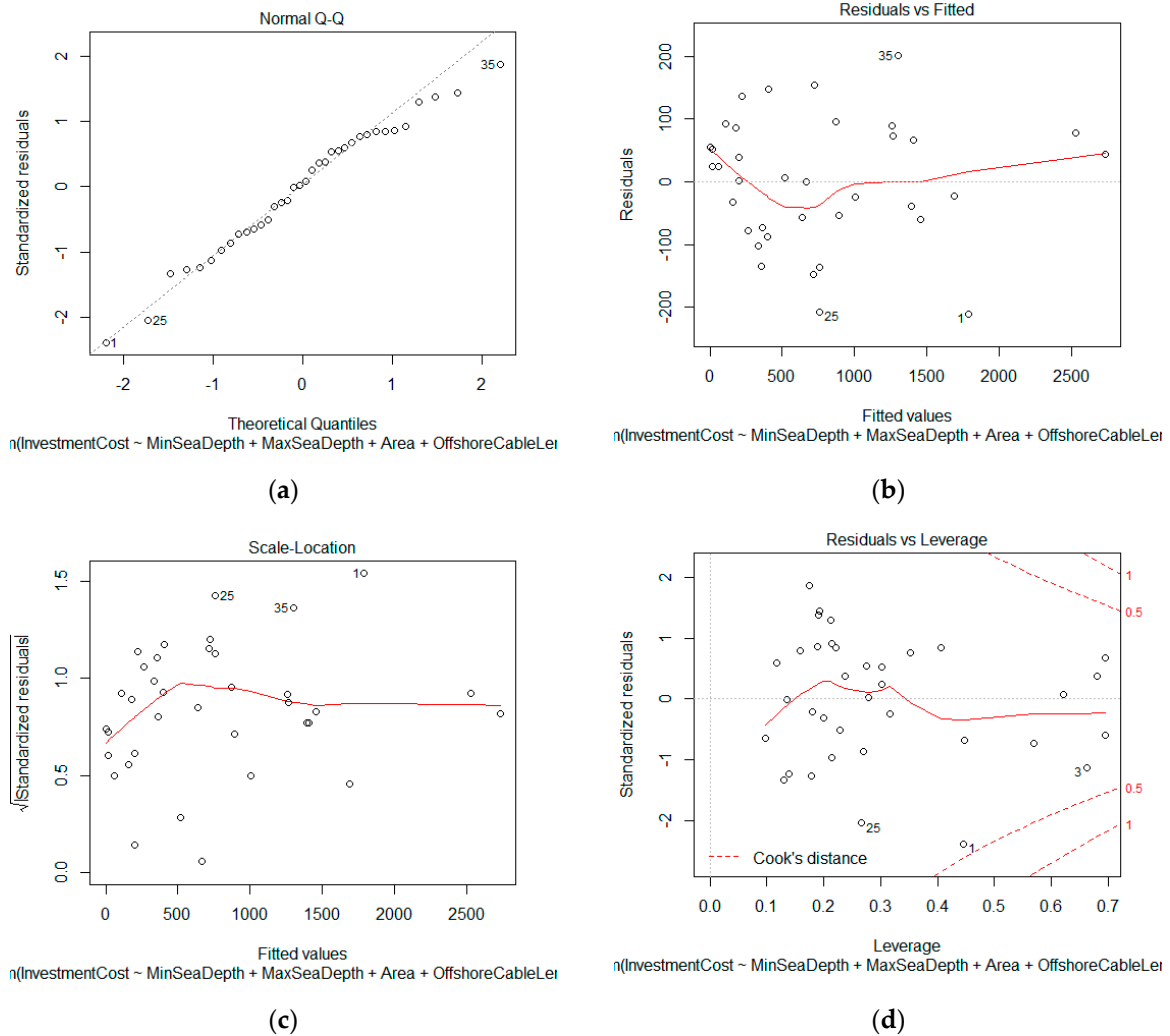


Figure 25. Multiple linear regression test for (a) normality, (b) linearity, (c) homoscedasticity, and (d) reliability of the 36 observations.

4.3.3. Model Selection

The multiple linear regression models with independent variables less than 5 *VIF* are shown in Table 1. There were 26 models generated and the other models with greater than 5 *VIF* were excluded since they indicate multicollinearity. Models 8, 9, 16, and 17 represent the plant capacity with the independent variable plant capacity itself. However, models 21, 22, 25, and 26 express the plant capacity in terms of number of turbines and capacity of the turbines. Since the models satisfied the four linear regression assumptions, the best model was chosen based on the criteria of R^2 and adjusted R^2 .

4.3.4. Adjusted R^2

The coefficient of determination of each multiple linear regression models is shown in Table 2. Among the models that satisfied the multiple linear regression assumptions, model 8 had the highest R^2 and adjusted R^2 with 97.40% and 96.75%, respectively. The model includes the independent variables minimum sea depth, area, offshore cable length, onshore cable length, port distance, capacity of the turbine, and plant capacity. This result implies that the model is a good fit for the observations considered.

Table 1. Variance inflation factor of the different models of independent variables.

Name	Individual Variables	Variable Removed	VIF
Model 8	MinSeaDepth + Area + OffshoreCableLength + OnshoreCableLength + PortDistance + CapTurbine + PlantCap	MaxSeaDepth, NumTurbine, InterArrayCableLength	MinSeaDepth = 1.966903, Area = 3.014808, OffshoreCableLength = 2.154003, OnshoreCableLength = 1.248556, PortDistance = 1.377031, CapTurbine = 1.402520, PlantCap = 3.646495
Model 9	MaxSeaDepth + Area + OffshoreCablelength + OnshoreCablelength + PortDistance + CapTurbine + PlantCap	MinSeaDepth, NumTurbine, InterArrayCablelength	MaxSeaDepth = 2.474813, Area = 3.207744, OffshoreCablelength = 2.009005, OnshoreCableLength = 1.229875, PortDistance = 1.493217, CapTurbine = 1.647750, PlantCap = 3.860488
Model 16	MinSeaDepth + OffshoreCablelength + OnshoreCablelength + PortDistance + CapTurbine + PlantCap	MaxSeaDepth, Area, InterArrayCablelength, NumTurbine	MinSeaDepth = 1.966185, OffshoreCablelength = 2.113326, OnshoreCablelength = 1.229009, PortDistance = 1.363429, CapTurbine = 1.402447, PlantCap = 1.558588
Model 17	MaxSeaDepth + OffshoreCablelength + OnshoreCablelength + PortDistance + Cap Turbine + PlantCap	MinSeaDepth, Area, InterArrayCablelength, NumTurbine	MaxSea Depth = 2.325112, OffshoreCableLength = 2.008671, OnshoreCablelength = 1.210969, PortDistance = 1.440038, CapTurbine = 1.622965, PlantCap = 1.486171
Model 21	MinSeaDepth + Area + OffshoreCableLength + OnshoreCablelength + PortDistance + NumTurbine + CapTurbine	PlantCap, MaxSeaDepth, InterArrayCableLength	MinSeaDepth = 1.948631, Area = 2.866016, OffshoreCableLength = 1.920793, OnshoreCablelength = 1.247374, PortDistance = 1.370884, NumTurbine = 3.566499, CapTurbine = 1.615025
Model 22	MaxSeaDepth + Area + OffshoreCablelength + OnshoreCablelength + PortDistance + NumTurbine + CapTurbine	PlantCap, MinSeaDepth, InterArrayCablelength	MaxSeaDepth = 2.422104, Area = 2.994082, OffshoreCablelength = 1.945860, OnshoreCablelength = 1.229641, PortDistance = 1.498961, NumTurbine = 3.730028, CapTurbine = 2.030133
Model 25	MinSeaDepth + OffshoreCablelength + OnshoreCablelength + PortDistance + NumTurbine + CapTurbine	PlantCap, MaxSeaDepth, Area, InterArrayCablelength	MinSeaDepth = 1.943687, OffshoreCablelength = 1.920234, OnshoreCableLength = 1.224317, PortDistance = 1.344159, NumTurbine = 1.603537, Cap Turbine = 1.528544
Model 26	MaxSeaDepth + OffshoreCablelength + OnshoreCablelength + PortDistance + NumTurbine + CapTurbine	PlantCap, MinSeaDepth, Area, InterArrayCablelength	MaxSeaDepth = 2.312621, OffshoreCablelength = 1.932499, OnshoreCablelength = 1.208195, PortDistance = 1.436073, NumTurbine = 1.538419, Cap Turbine = 1.841882

4.3.5. Investment Cost Regression Model 8

The results of the multiple linear regression coefficients of model 8 show the coefficients for the intercept, minimum sea depth, area, offshore cable length, onshore cable length, port distance, capacity of turbine, plant capacity at -163.0030 , 4.2942 , -3.9149 , 0.6885 , -2.0687 , 0.4292 , 13.3512 , and 5.0368 , respectively. These coefficients should be multiplied to the predictor variables to calculate the investment cost. The coefficient of the independent variable area and onshore cable length were negative, which implies that as these parameters increase, there is a decrease in investment cost. Further analysis was done to check the negative coefficients.

4.3.6. Checking of Investment Cost Regression Model 8

In the initial result of generating model 8, the normality was checked with all the independent variables combined. The normality of each independent variable was not taken into account in the analysis, and should be investigated. The Pearson correlation was added in the analysis, which checks the linear relationship between two independent variables [60].

Table 2. Coefficient of determination of the multiple linear regression models.

Name	Individual Variables	Variable Removed	Multiple R ²	Adj. R ²
Model 8	MinSeaDepth + Area + OffshoreCablelength + OnshoreCablelength + PortDistance + CapTurbine + PlantCap	MaxSeaDepth, NumTurbine, InterArrayCablelength	97.40%	96.75%
Model 9	MaxSeaDepth + Area + OffshoreCablelength + OnshoreCablelength + PortDistance + CapTurbine + PlantCap	MinSeaDepth, NumTurbine, InterArrayCablelength	97.24%	96.55%
Model 16	MinSeaDepth + OffshoreCablelength + OnshoreCablelength + PortDistance + CapTurbine+ Plantcap	MaxSeaDepth, Area, InterArrayCablelength, NumTurbine	96.42%	95.68%
Model 17	MaxSeaDepth + OffshoreCablelength + OnshoreCablelength + PortDistance + CapTurbine + PlantCap	MinSeaDepth, Area, InterArrayCablelength, NumTurbine	96.34%	95.59%
Model 21	MinSeaDepth + Area + OffshoreCablelength + OnshoreCablelength + PortDistance + NumTurbine + CapTurbine	PlantCap, MaxSeaDepth, InterArrayCablelength	91.80%	89.75%
Model 22	MaxSeaDepth + Area + OffshoreCablelength + OnshoreCablelength + PortDistance + NumTurbine+ CapTurbine	Plant Cap, MinSeaDepth, InterArrayCablelength	91.97%	89.96%
Model 25	MinSeaDepth + OffshoreCablelength + OnshoreCablelength + PortDistance + NumTurbine + CapTurbine	PlantCap, MaxSeaDepth, Area, InterArrayCablelength	91.61%	89.87%
Model 26	MaxSeaDepth + OffshoreCablelength + OnshoreCablelength + PortDistance + NumTurbine + CapTurbine	PlantCap, MinSeaDepth, Area, InterArrayCablelength	91.85%	90.16%

Upon checking the normality of each of the independent variables and dependent variable, only the maximum sea depth had a normal distribution. The independent variables minimum sea depth, area, offshore cable length, onshore cable length, inter-array cable length, port distance, number of turbine, capacity of turbine, and plant capacity were transformed to log normal to normalize the distribution. Observations 10 and 34 were omitted due to “-infinity” result in the transformation to log normal, and observation 23 was omitted due to multicollinearity. The dependent variable investment cost was also transformed to a log normal to normalize the distribution.

The Pearson correlation of all the independent variables with a value between -0.5 to 0.5 indicate that there was a medium correlation between each other, and this was the limit considered in the study. The independent variables that satisfied this criterion were minimum sea depth, port distance, capacity of turbine, and plant capacity and was labelled as model 27.

The normality, linearity, homoscedasticity and reliability were checked for the log normal of the independent variables minimum sea depth, port distance, capacity of turbine, and plant capacity, as shown in Figure 26a–d. As shown in Figure 26a, the majority of the observations followed a normal distribution, but points 4, 26, and 29 should be taken into account if it is within the Cook’s distance. The test for linearity showed that the observations resembled a linear pattern, as shown in Figure 26b. The observations followed homoscedasticity since the variance of errors were somehow similar across all independent variables, as seen in Figure 26c. For the reliability test in Figure 26d, all of the observations were within the Cook’s distance and implies that there was no multicollinearity. The four linear regression assumptions were all satisfied.

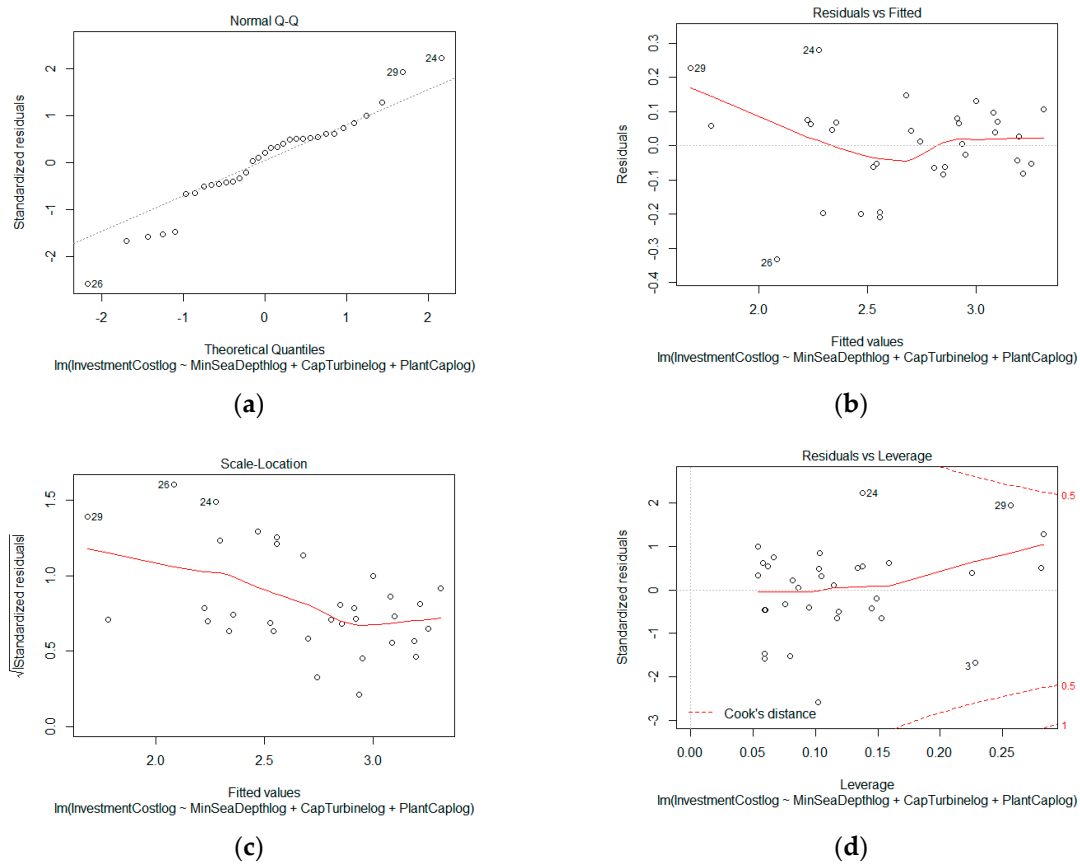


Figure 26. Multiple linear regression test for normality (a), linearity (b), homoscedasticity (c), and reliability (d) of model 27.

4.3.7. Selection of Investment Cost Regression Model

The multiple linear regression coefficients and R^2 of model 27 showed that the intercept value was 0.50223 with coefficients of 0.21401, 0.21699, and 0.88934 for the minimum sea depth, capacity of turbine, and plant capacity, respectively. Among the independent variables, the plant capacity had the highest influence since it had the highest coefficient. The coefficient of determination of the adjusted R^2 was 90.5%, which indicates that the model was still a good fit for the observations considered. On the other hand, the P-value for the turbine capacity was 0.27987, which was not less than 0.05 and means that it was not statistically significant. Therefore, the independent variable capacity of the turbine was omitted.

Model 28 is the regression model in which the capacity of the turbine was omitted from model 27. The four linear regression assumptions were satisfied by model 28. The multiple linear regression coefficients and R^2 of model 28 show that the intercept value was 0.61472 with coefficients of 0.25773 for the minimum sea depth and 0.87386 for the plant capacity. The plant capacity had the highest influence since it had the highest coefficient compared to the minimum sea depth. The coefficient of determination of the adjusted R^2 was 90.43%, which indicates that the model was still a good fit for the observations considered. This will be the regression model considered for acquiring the investment cost.

4.3.8. Multiple Linear Regression Model Validation

The multiple linear regression model 28 was validated using the other 24 observations that were not included in the model generation, as shown in Table 3. Model 28 had the least mean absolute percentage error (MAPE), which amounted to 11.33%. This means that there was an uncertainty of about 11.33% when predicting the investment cost using the

multiple linear regression model 8. In the sensitivity analysis, $\pm 11.33\%$ was analyzed for the investment cost.

Table 3. Validation of multiple linear regression model 28 using mean absolute percentage error.

	Actual Investment Cost (Million USD)	Predicted Investment Cost (Million USD)	Residuals	MAPE
1	1155.0303	1272.5352	-117.504902	0.10173318
2	1610.5574	1636.7401	-26.182712	0.01625693
3	1155.0303	1272.5352	-117.504902	0.10173318
4	1443.7878	1302.7241	141.063756	0.09770394
5	2079.0545	1988.9850	90.069423	0.04332230
6	2485.6456	2534.3208	-48.675219	0.01958253
7	1389.2856	1287.8844	101.401244	0.07298805
8	463.2340	334.1906	129.043308	0.27857048
9	1501.5393	1315.9762	185.563161	0.12358195
10	1355.8067	1331.0228	24.783887	0.01827981
11	1039.5272	996.5151	43.012121	0.04137662
12	2146.6939	1997.6728	149.021163	0.06941891
13	784.7990	717.1558	67.643246	0.08619180
14	740.0445	826.3828	-86.338284	0.11666634
15	1006.9377	922.6834	84.254318	0.08367381
16	578.7908	477.7106	101.080216	0.17464032
17	415.9957	424.3203	-8.324543	0.02001113
18	297.5603	401.2918	-103.731481	0.34860655
19	1030.7567	753.9011	276.855596	0.26859451
20	517.0838	606.1924	-89.108637	0.17232921
21	3163.5490	2602.6829	560.866112	0.17729016
22	492.4285	577.0530	-84.624516	0.17185138
23	458.1789	479.7112	-21.532298	0.04699540
24	898.0267	836.7780	61.248712	0.06820367
25	NA	NA	NA	0.11331676

4.4. Levelized Cost of Electricity

The levelized cost of electricity was computed by generating a polygon area in Arc GIS. The shape of the polygon was a rectangle, which is only a representative of the area of the offshore wind farm. This step was done to calculate the number of turbines based on the downwind and crosswind spacing factors of 10 and 5, respectively. The area generated in the map was 25.0372 km². There were two cases considered for the said area, namely, construction of 34 SWT-3.6-120 turbines with a plant capacity of 122.4 MW, as shown in Figure 27, and the construction of 31 6.2M126 turbines with a plant capacity of 192.2 MW, as shown in Figure 28. The levelized cost of electricity for the 34 SWT-3.6-120 turbines range from USD 156.829/MWh to USD 158.498/MWh. For the case with 31 6.2M126 turbines, the resulting LCOE ranged from USD 153.207/MWh to USD 154.995/MWh. The results were validated against the study done by Mattar [16] wherein the computed LCOE in Chile was within 72 USD/MWh to 322 USD/MWh using a V164 8.0 MW turbine. Another validation was done by applying the 41.2% capacity factor and 4.14 MW turbine with LCOE of USD 181/MWh in the model done by [61]. The resulting LCOE after applying the 41.2% capacity factor and the 4.14 MW in this study was between USD 179.19/MWh

and USD 183.63/MWh. The 6.2M126 turbine had lower *LCOE* because even though the investment cost was higher for this turbine, the plant capacity was greater in 6.2M126 than with SWT-3.6-120 given the same area. The plant capacity for 6.2M126 was 192.2 MW while SWT-3.6-120 had 122.4 MW.

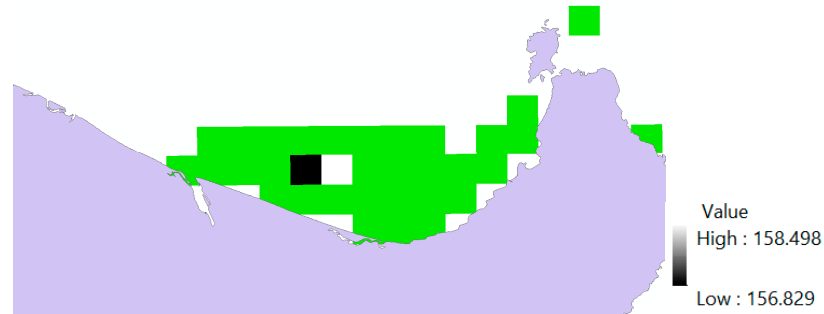


Figure 27. *LCOE* of SWT-3.6-120.

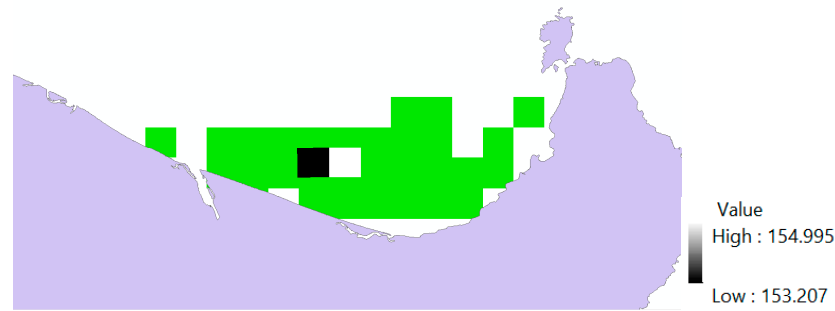


Figure 28. *LCOE* of 6.2M126.

The comparison of the *LCOE* of the SWT-3.6-120 and 6.2M126 in terms of plant capacity is shown in Figure 29. The parameters assumed for the basis of the *LCOE* were similar to the 25.0372 km² offshore wind farm in the north of Cagayan. The SWT-3.6-120 turbine had a lower *LCOE* compared to the 6.2M126 in all plant capacities from 0 MW to 1000 MW. The *LCOE* was lower in the case of SWT-3.6-120 since the 6.2M126 turbines have high investment cost and lower capacity factor. The *LCOE* had a similar behavior with exponential curves because even though the total life cycle cost increased with the increase in the plant capacity, the magnitude of the plant capacity as a divisor greatly affects the *LCOE*.

The comparison of the *LCOE* of the SWT-3.6-120 and 6.2M126 in terms of area can be seen in Figure 30. The parameters assumed for the basis of the *LCOE* were similar to the 25.0372 km² offshore wind farm in the north of Cagayan. The 6.2M126 turbine had lower *LCOE* compared to the SWT-3.120 in all areas from 0 km² to 150 km². Contrary to the results in the *LCOE* vs. plant capacity, the 6.2M126 turbine had less *LCOE* because even though its initial investment cost was higher compared with the SWT-3.6-120, the plant capacity of 6.2M126 was greater given the same area for both turbines.

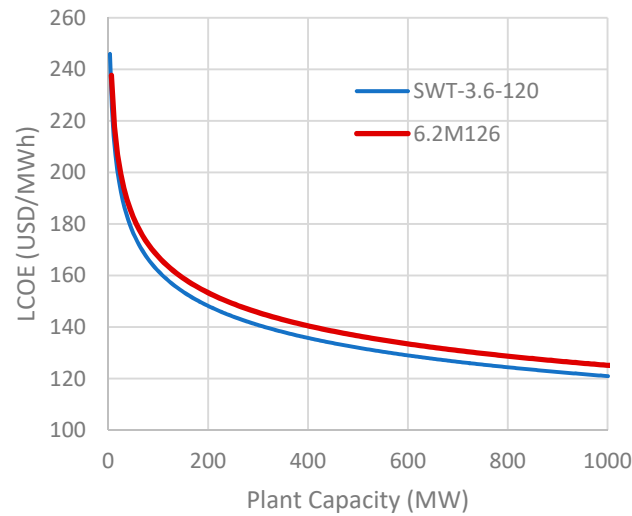


Figure 29. LCOE comparison of SWT-3.6-120 and 6.2M126 vs. plant capacity.

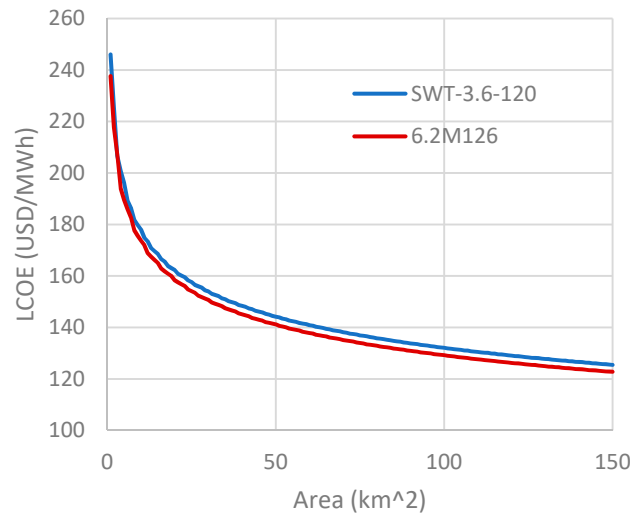


Figure 30. LCOE comparison of SWT-3.6-120 AND 6.2M126 vs. area.

4.5. Price of Electricity

The calculation for the price of electricity was based on the computation of the feed-in tariff for wind in the Philippines. It assumed an actual 200 MW onshore wind farm with its associated costs such as operation and maintenance cost and transmission interconnection cost. The feed-in-tariff for onshore wind farms was calculated to be PhP 7.40/kWh. The calculated offshore wind electricity price was PHP 8.028/kWh when the SWT-3.6-120 W was utilized, and a price of PHP 8.306/kWh when the 6.2M126 was used. The price of electricity from offshore wind farms is competitive against current feed-in-tariff because even though there is a higher investment cost for offshore wind farms, it was compensated for by its high capacity factor. The capacity factor assumed for the onshore wind farm was just 27.5%, while the calculated capacity factor for offshore wind farm in the study ranged from 45.80% to 47.91%.

4.6. Sensitivity Analysis

Figures 31 and 32 show the sensitivity analysis results for the LCOE when the SWT-3.6-120 and 6.2M126 were utilized, respectively. The base value for the LCOE for the SWT-3.6-120 and 6.2M126 turbines in the sensitivity analysis were USD 157.66/MWh and USD 154.1/MWh, respectively. The generated regression model had a mean absolute percentage

error of $\pm 11.33\%$, which was reflected in the investment cost of the sensitivity analysis. In the sensitivity analysis of the investment cost, there was a deviation of $\pm \text{USD}16.25/\text{MWh}$ to the *LCOE* for the SWT-3.6-120 turbine, and a deviation of $\pm \text{USD}17.91/\text{MWh}$ for the 6.2M126. The other parameters, namely, the capacity factor ($\pm 2\%$), weighted average cost of capital ($\pm 2\%$), cost of debt ($\pm 1\%$), cost of equity ($\pm 2\%$), and plant capacity ($\pm 5\%$) were also investigated to check how these parameters influence the *LCOE*. The basis in the adjustment of the parameters were small changes based on the nature of the parameters. As shown in Figures 31 and 32, the capacity factor had the highest influence among the other parameters, which had a deviation of $\pm \text{USD} 6.91/\text{MWh}$ for the SWT-3.6-120 and $\pm \text{USD} 6.54/\text{MWh}$ for 6.2M126. The weighted average cost of capital had a moderate influence on the *LCOE* with a $\pm \text{USD} 4.30/\text{MWh}$ for the SWT-3.6-120 and $\pm \text{USD} 4.19/\text{MWh}$ for the 6.2M126. The cost of debt, cost of equity, and plant capacity had less influence on the *LCOE*.

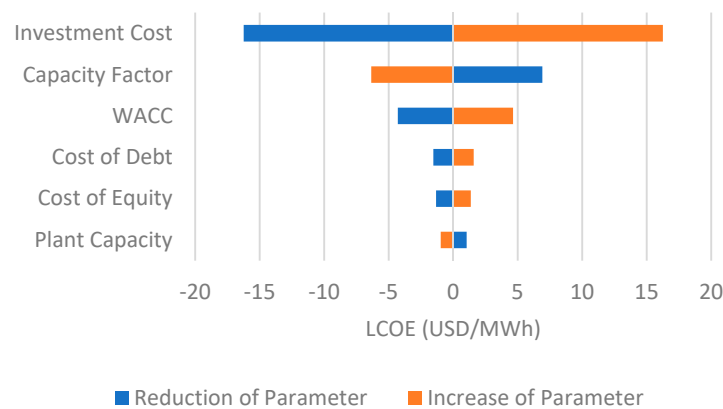


Figure 31. Sensitivity analysis of *LCOE* to different parameters (SWT-3.6-120).

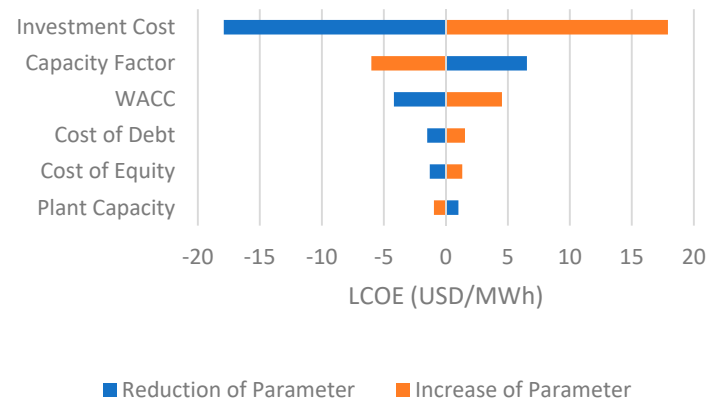


Figure 32. Sensitivity analysis of *LCOE* to different parameters (6.2M126).

The sensitivity analysis for the price of electricity from offshore wind in the Philippines using the SWT-3.6-120 and 6.2M126 turbines can be seen in Figures 33 and 34, respectively. The base offshore wind electricity prices for the SWT-3.6-120 and 6.2M126 in the analysis were PHP 8.028/kWh and PHP 8.306/kWh, respectively. The parameters considered were investment cost ($\pm 11.33\%$), capacity factor ($\pm 2\%$), plant capacity ($\pm 5\%$), weighted average cost of capital ($\pm 2\%$), cost of debt ($\pm 1\%$), and cost of equity ($\pm 2\%$). The 11.33% mean absolute percentage error of the regression model was checked in the sensitivity analysis while the other parameters were small changes based on the nature of the parameters. The $\pm 11.33\%$ adjustment in the investment cost resulted in a difference of $\pm \text{PHP} 0.91/\text{kWh}$ and $\text{PHP} 0.94/\text{kWh}$ to the offshore wind electricity price when using SWT-3.6-120 and 6.2M126, respectively. The plant capacity factor, capacity factor, and weighted average cost

of capital had moderate influence on the offshore wind electricity price. When adjusted to $\pm 5\%$ in the plant capacity, there was a difference of $\pm \text{PHP } 0.35/\text{kWh}$ and $\pm \text{PHP } 0.36/\text{kWh}$ to the electricity price when the SWT-3.6-120 and 6.2M126 were utilized, respectively. The adjustment of $\pm 2\%$ to the capacity factor resulted in a difference of $\pm \text{PHP } 0.35/\text{kWh}$ and $\pm \text{PHP } 0.38/\text{kWh}$ to the electricity price when utilizing the SWT-3.6-120 and 6.2M126, respectively. The adjustment of $\pm 2\%$ to the weighted average cost of capital resulted in a difference of $\pm \text{PHP } 0.18/\text{kWh}$ and $\pm \text{PHP } 0.19/\text{kWh}$ to the electricity price when the SWT-3.6-120 and 6.2M126 were utilized, respectively. The other parameters, namely, cost of debt and cost of equity had low influence on electricity price.

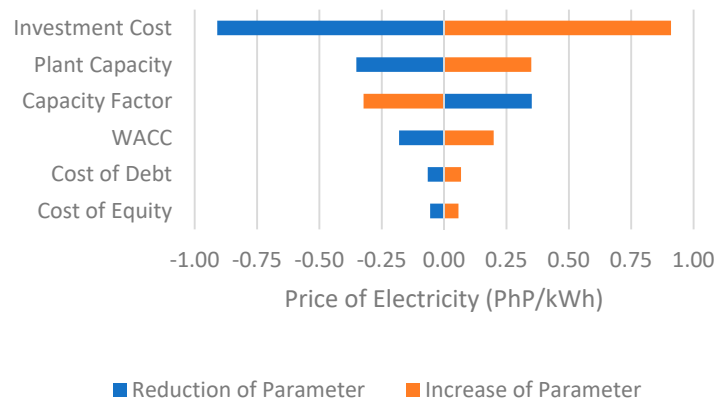


Figure 33. Sensitivity analysis of electricity price to different parameters (SWT-3.6-120).

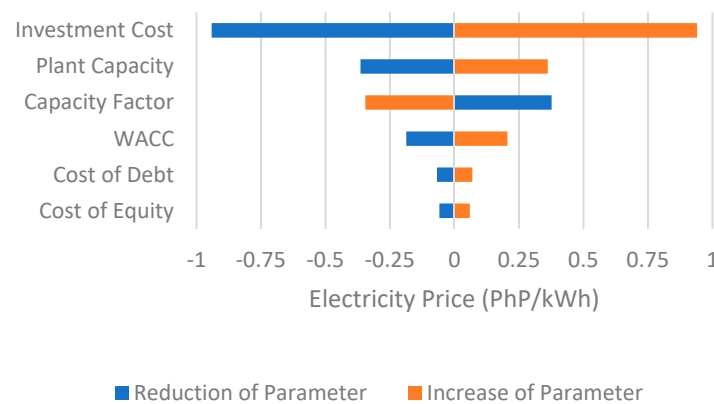


Figure 34. Sensitivity analysis of electricity price to different parameters (6.2M126).

5. Conclusions and Recommendations

The technical and economic assessments for emerging renewable energy technologies, specifically offshore wind energy, are critical for their improvement and deployment. These assessments serve as one of the main bases for the construction of offshore wind farms, which would be beneficial to the countries gearing toward a sustainable future such as the Philippines.

Two popular wind turbines were studied in the technical analysis. The capacity factor was calculated for both the Siemens SWT-3.6-120 and the Senvion 6.2M126 turbines. Results showed that the greatest values were in the northern parts of Ilocos Norte with a maximum of 62.60% for the Siemens turbine and 64.79% for the Senvion turbine. Two other locations also presented favorable values of capacity factors with the northern parts of Occidental Mindoro registering maximum values of 60.92% for the Siemens turbine and 62.60% for the Senvion turbine, while the southeastern parts of Oriental Mindoro recorded highest values of 59.52% for the Siemens turbine and 62.60% for the Senvion turbine. These locations were eventually excluded due to technical, political, and social restrictions. After masking out

all exclusion criteria, the areas most suitable for development of offshore wind farms were north of Cagayan, west of Rizal, north of Camarines Sur, north of Samar, southwest of Masbate, Dinagat Island, Guimaras, and northeast of Palawan. To carry out the economic analysis, the north of Cagayan was chosen since this area recorded the greatest capacity factor from the list of potential sites.

In the economic assessment of the study, a multiple linear regression of the parameters of 33 actual offshore wind farms from 2008 to 2018 were considered. The parameters considered for the regression model were minimum and maximum sea depth, area, offshore cable length, onshore cable length, inter-array cable length, port for O&M, distance from port, turbine model, number of turbines, turbine capacity, plant capacity, and investment cost to model the investment cost of offshore wind farms. When the four linear regression assumptions were investigated, namely, normality, linearity, homoscedasticity, and reliability of measurement, the model generated consisted of minimum sea depth, turbine capacity, and the plant capacity. The regression model generated had an adjusted R^2 equal to 90.43%, which implies that it fits the model of the actual investment costs at the 95% confidence level. The regression model was also validated by applying it to 24 actual offshore wind farms, and the mean absolute percentage error of the regression model was calculated to be 11.33%, which means that there was 11.33% uncertainty when predicting the investment cost.

The results of the combined technical and economic assessment were reflected in the calculated *LCOE* and price of electricity of offshore wind farms in the Philippines. The *LCOE* calculated were USD 157.66/MWh and USD 154.1/MWh when using the SWT-3.6-120 and 6.2M126 turbines, respectively. This *LCOE* was comparable in the techno-economic study done for Chile with a range of *LCOE* from USD 72/MWh to USD 322/MWh. Another validation was done by applying the 41.2% capacity factor and 4.14 MW turbine in the model of the NREL which resulted in USD 181/MWh, and the calculated *LCOE* of the economic model resulted in USD 179.19/MWh and USD 183.63/MWh. The price of electricity was compared with the calculation for the feed in tariff of 200 MW onshore wind farm in the Philippines. The calculated price of electricity from offshore wind were PHP 7.64/kWh and PHP 8.028/kWh when the SWT-3.6-120 W was utilized, and a price of PHP 8.306/kWh when the 6.2M126 was utilized. The price calculated was competitive against the onshore wind farm feed-in tariff of PHP 7.40/kWh.

The *LCOE* of the SWT-3.6-120 and 6.2M126 were compared with each other through a scatter plot of plant capacity and area. The *LCOE* was lower for the SWT-3.6-120 given the same power plant capacity because the investment cost was greater with 6.2M126. However, the 6.2M126 had lower *LCOE* when the area for both turbines were the same due to higher plant capacity.

Based on the sensitivity analysis, the parameters that may greatly influence the *LCOE* are investment cost, capacity factor, and weighted average cost of capital for each instance when the SWT-3.6-120 and 6.2M126 were used. In the electricity price from offshore wind, the results showed that the investment cost, plant capacity, weighted average cost of capital, and the capacity factors were the most influential parameters.

However, it should be taken into account that the estimated investment cost for a 200 MW offshore wind farm is approximately USD 862.653 million while the investment cost for a 200 MW onshore wind farm amounts to USD 466 million. The offshore wind farm investment is approximately twice that of an onshore wind farm, and a possible option for pursuing offshore wind farms is through financing.

The future recommendation for this study is the consideration of the general soil characteristics of the potential sites for the construction of offshore wind farms that were not included in the study due to a lack of available data. Investigation of floating offshore wind farms in the Philippines can also be done with the methodology discussed in the study.

Author Contributions: Conceptualization, G.L.D.M. and M.-A.M.T.-K.; Methodology, G.L.D.M., M.-A.M.T.-K. and L.A.M.D.; Software, G.L.D.M.; Validation, G.L.D.M. and M.-A.M.T.-K.; Formal

analysis, G.L.D.M.; Writing—original draft preparation, G.L.D.M., M.-A.M.T.-K. and L.A.M.D.; Writing—review and editing, L.A.M.D.; Visualization, G.L.D.M.; Supervision, M.-A.M.T.-K. and L.A.M.D.; Funding acquisition, L.A.M.D. All authors have read and agreed to the published version of the manuscript.

Funding: The APC was funded by the Department of Science and Technology (DOST) Engineering Research and Development for Technology (ERDT) Program.

Acknowledgments: The authors thank the Department of Science and Technology (DOST) Engineering Research and Development for Technology (ERDT) Program for the scholarship provided to the student to conduct this study.

Conflicts of Interest: The authors declare no conflict of interest.

References

1. GOV.PH. *An Act Promoting the Development, Utilization and Commercialization of Renewable Energy Resources and for Other Purposes*; Republic Act No. 9513; GOV.PH: Metro Manila, Philippines, 2008.
2. GOV.PH. *Department of Energy, Department Circular DC2009-05-0008*; Rules and Regulations Implementing Republic Act 9513; GOV.PH: Metro Manila, Philippines, 2009.
3. Department of Energy—Electric Power Industry Management Bureau. *2015 Philippine Power Situation Report*; Department of Energy: Taguig, Philippines, 2016.
4. Perveen, R.; Kishor, N.; Mohanty, S. Off-shore wind farm development: Present status and challenges. *Renew. Sustain. Energy Rev.* **2014**, *29*, 780–792. [[CrossRef](#)]
5. Richts, C.; Jansen, M.; Siefert, M. Determining the Economic Value of Offshore Wind Power Plants in the Changing Energy System. *Energy Procedia* **2015**, *80*, 422–432. [[CrossRef](#)]
6. Department of Energy. *List of Existing Power Plants in Luzon as of June 2016*; Department of Energy: Taguig, Philippines, 2016.
7. Department of Energy. *List of Existing Power Plants in Visayas as of June 2016*; Department of Energy: Taguig, Philippines, 2016.
8. Wang, S.; Wang, S. Impacts of wind energy on environment: A review. *Renew. Sustain. Energy Rev.* **2015**, *49*, 437–443. [[CrossRef](#)]
9. Bakker, R.; Pedersen, E.; Van Den Berg, G.; Stewart, R.; Lok, W.; Bouma, J. Impact of wind turbine sound on annoyance, self-reported sleep disturbance and psychological distress. *Sci. Total Environ.* **2012**, *425*, 42–51. [[CrossRef](#)]
10. Green, R.; Vasilakos, N. The economics of offshore wind. *Energy Policy* **2011**, *39*, 496–502. [[CrossRef](#)]
11. Zerrahn, A. Wind Power and Externalities. *Ecol. Econ.* **2017**, *141*, 245–260. [[CrossRef](#)]
12. Pineda, I.; Tardieu, P. *Wind in Power 2017 Annual Combined Onshore and Offshore Wind Energy Statistics*; WindEurope: Brussels, Belgium, 2018.
13. Rodrigues, S.; Restrepo, C.; Kontos, E.; Teixeira Pinto, R.; Bauer, P. Trends of offshore wind projects. *Renew. Sustain. Energy Rev.* **2015**, *49*, 1114–1135. [[CrossRef](#)]
14. Shi, W.; Park, H.; Chung, C.; Kim, Y. Comparison of Dynamic Response of Monopile, Tripod and Jacket Foundation System for a 5-MW Wind Turbine. In *Twenty-First (2011) International Offshore and Polar Engineering Conference*; International Society of Offshore and Polar Engineers: Maui, Hawaii, 2011.
15. Arapogianni, A.; Genachte, A. *Deep Water—The Next Step for Offshore Wind Energy*; European Wind Energy Association: Brussels, Belgium, 2013.
16. Mattar, C.; Guzmán-Ibarra, M. A techno-economic assessment of offshore wind energy in Chile. *Energy* **2017**, *133*, 191–205. [[CrossRef](#)]
17. Nagababu, G.; Kachhwaha, S.; Naidu, N.; Savsani, V. Application of reanalysis data to estimate offshore wind potential in EEZ of India based on marine ecosystem considerations. *Energy* **2017**, *118*, 622–631. [[CrossRef](#)]
18. Khraiwish Dalabeeh, A. Techno-economic analysis of wind power generation for selected locations in Jordan. *Renew. Energy* **2017**, *101*, 1369–1378. [[CrossRef](#)]
19. Schweizer, J.; Antonini, A.; Govoni, L.; Gottardi, G.; Archetti, R.; Supino, E.; Berretta, C.; Casadei, C.; Ozzi, C. Investigating the potential and feasibility of an offshore wind farm in the Northern Adriatic Sea. *Appl. Energy* **2016**, *177*, 449–463. [[CrossRef](#)]
20. Cavazzi, S.; Dutton, A. An Offshore Wind Energy Geographic Information System (OWE-GIS) for assessment of the UK's offshore wind energy potential. *Renew. Energy* **2016**, *87*, 212–228. [[CrossRef](#)]
21. Mahdy, M.; Bahaj, A. Multi criteria decision analysis for offshore wind energy potential in Egypt. *Renew. Energy* **2018**, *118*, 278–289. [[CrossRef](#)]
22. Hornyak, T. Here's What To Takes To Lay Google's 9000 km Undersea Cable. 2015. Available online: <https://www.infoworld.com/article/2947900/networking/heres-what-to-takes-to-lay-googles-9000km-undersea-cable.html> (accessed on 11 April 2018).
23. Submarine Cable Map. 2017. Available online: <https://www.submarinecablemap.com/> (accessed on 15 April 2018).
24. Crevoisier, T. Philippines, Operational Ferry Routes. 2014. Available online: https://geonode.wfp.org/layers/geonode:phl_trs_waterways_wfp#more (accessed on 11 May 2018).
25. GOV.PH. *An Act Providing for the Establishment and Management of National Integrated Protected Areas System, Defining Its Scope and Coverage, and for Other Purposes*; Republic Act No. 7586; GOV.PH: Metro Manila, Philippines, 1992.

26. UNEP-WCMC. Protected Area Profile for Philippines from the World Database of Protected Areas. 2018. Available online: <https://www.protectedplanet.net/country/PH> (accessed on 15 April 2018).
27. Weeks, R.; Russ, G.; Alcalá, A.; White, A. Effectiveness of Marine Protected Areas in the Philippines for Biodiversity Conservation. *Conserv. Biol.* **2010**, *24*, 531–540. [[CrossRef](#)]
28. Cabral, R.; Geronimo, R. How important are coral reefs to food security in the Philippines? Diving deeper than national aggregates and averages. *Mar. Policy* **2018**, *91*, 136–141. [[CrossRef](#)]
29. Gomez, E.; Aliño, P.; Yap, H.; Licuanan, W. A review of the status of Philippine reefs. *Mar. Pollut. Bull.* **1994**, *29*, 62–68. [[CrossRef](#)]
30. ReefBase. A Global Information System for Coral Reefs. 2018. Available online: <http://www.reefbase.org> (accessed on 1 May 2018).
31. 5th Philippine Energy Contracting Round (PERC5). 5Th Philippine Energy Contracting Round Petroleum Areas for Offer Figures and Maps. 2014. Available online: <https://www.doe.gov.ph/figures-and-maps-petroleum> (accessed on 15 May 2018).
32. Philippine Bathymetry Grid. General Bathymetric Chart of the Oceans (GEBCO). 2018. Available online: <https://www.gebco.net/> (accessed on 20 April 2018).
33. Philippine Transmission Lines. Renewable Energy Data Explorer, National Renewable Energy Laboratory. 2018. Available online: <https://www.re-explorer.org/> (accessed on 27 March 2018).
34. Worsnop, R.; Lundquist, J.; Bryan, G.; Damiani, R.; Musial, W. Gusts and shear within hurricane eyewalls can exceed offshore wind turbine design standards. *Geophys. Res. Lett.* **2017**, *44*, 6413–6420. [[CrossRef](#)]
35. Philippines: Hazard Profile. UN Office for the Coordination of Humanitarian Affairs. 2017. Available online: <https://reliefweb.int/map/philippines/philippines-hazard-profile-jan-2017> (accessed on 1 March 2018).
36. Black, M.; Willoughby, H. The Concentric Eyewall Cycle of Hurricane Gilbert. *Mon. Weather Rev.* **1992**, *120*, 947–957. [[CrossRef](#)]
37. Takagi, H.; Wu, W. Maximum wind radius estimated by the 50 kt radius: Improvement of storm surge forecasting over the western North Pacific. *Nat. Hazards Earth Syst. Sci.* **2016**, *16*, 705–717. [[CrossRef](#)]
38. Matsunobu, T.; Inoue, S.; Tsuji, Y.; Yoshida, K.; Komatsuzaki, M. Seismic Design of Offshore Wind Turbine Withstands Great East Japan Earthquake and Tsunami. *J. Energy Power Eng.* **2014**, *8*, 2039–2044.
39. Truelsen, C. Offshore Wind Turbines Must Withstand Typhoons and Earthquakes in Taiwan. Available online: <https://www.niras.com/projects/offshore-jacket-design/> (accessed on 10 April 2018).
40. Chiaradonna, A.; Tropeano, G.; Donofrio, A.; Silvestri, F. Interpreting the deformation phenomena of a levee damaged during the 2012 Emilia earthquake. *Soil Dyn. Earthq. Eng.* **2019**, *124*, 389–398. [[CrossRef](#)]
41. Bird, L.; Cochran, J.; Wang, X. *Wind and Solar Energy Curtailment: Experience and Practices in the United States*; NREL/TP-6A20-60983; National Renewable Energy Laboratory: Golden, CO, USA, 2014.
42. Bird, L.; Lew, D.; Milligan, M.; Carlini, E.; Estanqueiro, A.; Flynn, D.; Gomez-Lazaro, E.; Holttinen, H.; Menemenlis, N.; Orths, A.; et al. Wind and solar energy curtailment: A review of international experience. *Renew. Sustain. Energy Rev.* **2016**, *65*, 577–586. [[CrossRef](#)]
43. Ang, M.R.C.O.; Blanco, A.C. *Philippine Renewable Energy Resource Mapping from LiDAR Surveys (REMap) Project Terminal Report*; UP TCAGP: Quezon City, Philippines, 2017.
44. Murthy, K.; Rahi, O. A comprehensive review of wind resource assessment. *Renew. Sustain. Energy Rev.* **2017**, *72*, 1320–1342. [[CrossRef](#)]
45. Celik, A. A statistical analysis of wind power density based on the Weibull and Rayleigh models at the southern region of Turkey. *Renew. Energy* **2004**, *29*, 593–604. [[CrossRef](#)]
46. Siemens AG. Thoroughly Tested, Utterly Reliable Siemens Wind Turbine SWT-3.6-120. 2011. Available online: https://www.siemens.com.tr/i/Assets/Enerji/yenilenebilir_enerji/E50001-W310-A169-X-4A00_WS_SWT_3-6_120_US.pdf (accessed on 16 March 2018).
47. Senvion GmbH. 3.2M126 Wind Turbine 6.2MW. 2017. Available online: <https://www.senvion.com/global/en/products-services/wind-turbines/6xm/62m126/> (accessed on 17 March 2018).
48. Tegen, S.; Lantz, E.; Hand, M.; Maples, B.; Smith, A.; Schwabe, P. *2011 Cost of Wind Energy Review*; NREL/TP-5000-56266; National Renewable Energy Laboratory: Golden, CO, USA, 2013.
49. Nagababu, G.; Kachhwaha, S.; Savsani, V. Estimation of technical and economic potential of offshore wind along the coast of India. *Energy* **2017**, *138*, 79–91. [[CrossRef](#)]
50. Sheridan, B.; Baker, S.; Pearre, N.; Firestone, J.; Kempton, W. Calculating the offshore wind power resource: Robust assessment methods applied to the U.S. Atlantic Coast. *Renew. Energy* **2012**, *43*, 224–233. [[CrossRef](#)]
51. Gonzalez-Rodriguez, A. Review of offshore wind farm cost components. *Energy Sustain. Dev.* **2017**, *37*, 10–19. [[CrossRef](#)]
52. Li, D.; Geyer, B.; Bisling, P. A model-based climatology analysis of wind power resources at 100-m height over the Bohai Sea and the Yellow Sea. *Appl. Energy* **2016**, *179*, 575–589. [[CrossRef](#)]
53. Schwanitz, V.; Wierling, A. Offshore wind investments—Realism about cost developments is necessary. *Energy* **2016**, *106*, 170–181. [[CrossRef](#)]
54. Montgomery, D.; Runger, G. *Applied Statistics and Probability for Engineers*, 3rd ed.; John Wiley & Sons, Inc.: Danvers, MA, USA, 2003.
55. De Myttenaere, A.; Golden, B.; Le Grand, B.; Rossi, F. Mean Absolute Percentage Error for regression models. *Neurocomputing* **2016**, *192*, 38–48. [[CrossRef](#)]

-
56. Osborne, J.W.; Waters, E. Four assumptions of multiple regression that researchers should always test. *Pract. Assess. Res. Eval.* **2002**, *8*, 2.
 57. Kim, B. Understanding Diagnostic Plots for Linear Regression Analysis University of Virginia Library Research Data Services + Sciences. Data.library.virginia.edu. 2015. Available online: <https://data.library.virginia.edu/diagnostic-plots/> (accessed on 3 May 2018).
 58. Ioannou, A.; Angus, A.; Brennan, F. Stochastic Prediction of Offshore Wind Farm LCOE through an Integrated Cost Model. *Energy Procedia* **2017**, *107*, 383–389. [[CrossRef](#)]
 59. Möller, B.; Hong, L.; Lonsing, R.; Hvelplund, F. Evaluation of offshore wind resources by scale of development. *Energy* **2012**, *48*, 314–322. [[CrossRef](#)]
 60. Cohen, J. *Statistical Power Analysis for the Behavioral Sciences*, 2nd ed.; Erlbaum: Hillsdale, NJ, USA, 1987.
 61. Mone, C.; Hand, M.; Bolinger, M.; Rand, J.; Heimiller, D.; Ho, J. *2015 Cost of Wind Energy Review*; NREL/TP-6A20-66861; National Renewable Energy Laboratory: Golden, CO, USA, 2017.